Reviewed Preprint
v1 • April 15, 2026
Not revised

For correspondence:
zhangqi@human.tsukuba.ac.jp

Cross-Species BAC Transgenesis Reveals Long-Range Regulation Drives Variation in Brain Oxytocin Receptor Expression and Social Behaviors

Mina Tsukamoto[1], Luis AE Nagai[2], Kiyoshi Inoue[3], Lenin C Kandasamy[1], Maria F Pires[1], Minsoo Shin[1], Yutaro Nagasawa[1], Tsetsegee Sambuu[1], Kenta Nakai[4], Shigeyoshi Itohara[5], Larry J Young[3,6,7,#], Qi Zhang[1,5,6,8]

[1]Laboratory for Social Neural Networks, Faculty of Human Sciences, University of Tsukuba, Tsukuba, Japan • [2]Laboratory of Computational Genomics, Institute for Quantitative Biosciences, The University of Tokyo, Tokyo, Japan • [3]Center for Translational Social Neuroscience, Emory National Primate Research Center, Emory University, Atlanta, United States • [4]Laboratory of Functional Analysis in silico, Human Genome Center, The University of Tokyo, Tokyo, Japan • [5]Laboratory for Behavioral Genetics, CBS, RIKEN, Wako, Japan • [6]Center for Social Neural Networks, Faculty of Human Sciences, University of Tsukuba, Tsukuba, Japan • [7]Department of Psychiatry and Behavioral Science, Emory University, Atlanta, United States • [8]Institute for Glyco-core Research, Tokai National Higher Education and Research System, Gifu University, Gifu, Japan

[#] Deceased in March, 2024. We dedicate this work to the memory of Dr. Larry J. Young, whose encouragement and unwavering support helped our team persevere through challenges.

Classification: Biological Science: Neuroscience

Competing interests: No competing interests declared

Funding: See page 23

Reviewing editor: Bianca Jones Marlin, Howard Hughes Medical Institute, United States

eLife Assessment

This study provides **important** insights into how species-specific variation in oxytocin receptor regulatory architecture contributes to diversity in brain expression patterns and social behaviors. By generating multiple BAC transgenic mouse lines carrying the prairie vole oxytocin receptor locus and combining anatomical, molecular, behavioral, and chromatin-structure analyses, the authors present **convincing** evidence that distal regulatory elements constrain peripheral expression while permitting brain expression aligned with behavior. This study provides an experimental framework and a resource that are of value for dissecting how regulatory variation in neuromodulatory systems contributes to species differences in social behavior. This work will be of interest to those interested in social behavior, oxytocin, neuromodulation, and related conditions.

https://doi.org/10.7554/eLife.109080.1.sa2

Abstract

Although oxytocin (OXT) exhibits a highly conserved neuroanatomical pattern among vertebrates, the distribution of OXT receptor (OXTR) in brain varies considerably across species and is associated with species-typical social behavior. To investigate the genomic basis of the phylogenetic plasticity in brain *Oxtr* expression and its social behavioral consequences, we generated transgenic mice carrying a bacteria artificial chromosome (BAC) harboring the entire prairie vole *Oxtr* locus and flanking intergenic regulatory regions. We established eight independent "volized" mouse lines expressing prairie vole *Oxtr* (pv*Oxtr*). Strikingly, despite conserved *Oxtr* expression in mammary gland of all transgenic mouse lines, each line displayed a unique pattern of brain expression distinct from both mice and prairie voles. Together with topologically associating domain (TAD) structure analysis with mouse genome, our findings suggest that unlike *Oxt*, *Oxtr* expression patterns in brain, involve contributions of distal regulatory elements beyond the BAC insert. In contrast, *Oxtr* expression in peripheral tissues appears resistant to such distal influences. Moreover, the "volized" mouse lines with different brain *Oxtr* expression patterns showed differences in partner preference and maternal behaviors, providing direct functional evidence that variation in brain *Oxtr* expression can drive differences

in social behaviors. We propose that brain *Oxtr* expression is transcriptionally sensitive to long-range interactions with distal genomic elements, rendering it more susceptible to diverse regulatory influences. This supports a model in which regulatory flexibility facilitates the evolutionary diversification of social behavior, while maintaining essential peripheral *Oxtr* expression.

Highlights

Unlike essential physiological phenomenon including feeding, sex, parturition and lactation, which are conserved across mammalian species, there is extraordinary diversity of social behaviors between and within species. Comparative studies across species suggest that variation in brain oxytocin receptor expression may mediate diversity in social behavior. Subtle variations in human oxytocin receptor sequence have been related to psychiatric phenotypes. Our studies suggest that the oxytocin receptor gene is hypersensitive to long-distance sequence variation, as revealed by differential expression patterns when the BAC transgene was inserted at different genomic sites, leading to variability in brain expression and social behavior. This research provides new insights into the evolvability of genes producing diversity in social behaviors, which allows efficient adaptation of animals to variable environment. Furthermore, our cross-species study demonstrates that diversity in brain OXTR expression patterns leads to variation in mouse social behaviors. The “volized” *Oxtr* mouse lines generated here present a valuable resource for further exploring OXTR expression regulation and neural circuits/networks mediating social behavioral variability.

Introduction

Brain oxytocin receptors (OXTR) regulate a wide range of social behaviors including social recognition, maternal care, social bonding, empathy related behaviors, and aggression (Froemke & Young, 2021; Jurek & Neumann, 2018; Rigney, de Vries, Petrulis, & Young, 2022). In contrast to sex steroid receptors, which have highly conserved brain expression patterns across species, OXTR shows remarkable inter- and intra-species variation in brain distribution (Froemke & Young, 2021; Larry J. Young & Zhang, 2021). For example, monogamous prairie voles have a brain OXTR distribution in cortex, striatum and amygdala that is significantly distinct from promiscuous montane voles and laboratory rats and mice(Larry J. Young & Zhang, 2021). Furthermore, there is robust individual variation in brain OXTR expression among prairie voles that is associated with single nucleotide polymorphisms (SNPs) in the OXTR locus (*Oxtr*), and this variation predicts pair bonding behavior and resilience to early life social neglect (Ahern, Olsen, Tudino, & Beery, 2021; Barrett, Arambula, & Young, 2015; King, Walum, Inoue, Eyrich, & Young, 2016; Ross et al., 2009). Different species of primates also differ in brain OXTR distribution (Rogers Flattery et al., 2022), and SNPs in the human OXTR have been linked to variation in social function (Skuse et al., 2014; Theofanopoulou, Andirkó, Boeckx, & Jarvis, 2022). Thus, variation in OXTR distribution in brain likely constitutes a mechanism for the emergence of diverse social traits, potentially including psychiatric endophenotypes.

The evolution of gene expression patterns could be mediated by *cis* (via linked polymorphisms) or *trans* (through diffusible products of distal genes, e.g., transcription factors) changes, as a result of adaptation to the environment (Mack, Campbell, & Nachman, 2016; Osada, Miyagi, & Takahashi, 2017; Shi et al., 2012). *Cis*-regulatory differences are more commonly responsible for adaptive evolution and interspecific divergence (Signor & Nuzhdin, 2018). To explore the transcriptional mechanisms giving rise to species-specific *Oxtr* expression and social behavior, we created transgenic mice using a prairie vole *Oxtr* (pv*Oxtr*) bacterial artificial chromosome (BAC). The BAC construct covers the full coding sequence, introns and the entire intergenic region of the pv*Oxtr* with its neighboring genes. We expected that our BAC construct accommodates all the critical regulatory sequences responsible for species- and tissue-specific expression, so that pv*Oxtr* transgenic mice would express brain pv*Oxtr* in a prairie vole-like pattern, largely independent of integration sites. Then we would examine if our transgenic mouse could develop social behaviors similar to that of prairie vole.

We generated eight pv*Oxtr* mouse lines with successful germline transmission. Each line, defined by a distinct BAC integration site, exhibited a unique brain-specific expression pattern of *Oxtr*, distinct from both wildtype mice and prairie voles. Notably, *Oxtr* expression in the mammary gland was conserved across all lines. This suggests that brain, but not mammary gland, expression of *Oxtr* is shaped by distal regulatory elements beyond the BAC insert. These findings imply that evolution has placed brain *Oxtr* expression under more complex regulatory control, likely to accommodate the diversification of social behaviors, whereas mammary gland expression is maintained by simpler mechanisms supporting conserved lactation functions. Furthermore, behavioral assays revealed line-specific differences in partner preference and maternal behaviors.

The 3D architecture of the genome, segregated into TADs demarcated by CCCTC-binding factor (CTCF), crucially influences gene expression. Through the loop extrusion model, CTCF enables interactions between distant regulatory elements, facilitating precise gene regulation, which ultimately shapes an organism's phenotype and behavior(Wendt et al., 2008). Hi-C data provide a genome-wide view of chromosome conformation in multiple layers, such as compartments, TADs, and loops(Gibcus & Dekker, 2013; Lieberman-Aiden et al., 2009). Our TAD analysis with Hi-C database showed a clear difference exists between the 3D structures of *Oxt* and *Oxtr* gene, and a clear difference exists between the 3D structures of brain tissue *Oxtr* and peripheral tissue *Oxtr*, suggesting that Oxtr expression patterns in brain depends on contributions from very distal sequences. These results provide important clues to understand the genetic mechanism underlying species differences in brain gene expression.

Together, our data demonstrate that transcriptional redistribution of brain *Oxtr* can drive variation in social and parental behaviors—variation that natural selection could act upon in specific ecological contexts. Our results also offer insights into the genetic mechanisms underlying species-specific brain gene expression.

Results

Creation of the pv*Oxtr-P2A-Cre* BAC transgenic mice

BAC vectors can accommodate dispersed cis-regulatory elements across large regions of genome. Transgene expression from BAC constructs are generally resistant to insertion position effects (Suster, Abe, Schouw, & Kawakami, 2011) due to both the large spans of insulating genetic material which protect the transgene cassette from the influence of the chromosomal environment, and through the inclusion of necessary regulatory elements such as enhancers, silencers, locus control regions, and matrix attachment regions (Beil, Fairbairn, Pelczar, & Buch, 2012; Bian & Belmont, 2010). Large-scale screening of CNS gene expression in BAC transgenic mice by the GENSAT (Gene Expression Nervous System Atlas) Project found that more than 85% of BACs express reproducibly in multiple independent transgenic lines and reporter gene expression faithfully recapitulates endogenous gene expression patterns (Gerfen, Paletzki, & Heintz, 2013; Heintz, 2004; Schmidt, Kus, Gong, & Heintz, 2013). Indeed, reproducible expression from mouse BAC vectors has been achieved for more than 500 genes (Gerfen et al., 2013; Heintz,

2004; Schmidt et al., 2013). Few that don't express reproducibly are influenced by variation in BAC copy number and insertion sites (S. Gong et al., 2007). BAC engineering has also been used to mediate cross-species transgene expression. A large number of mouse models of human dominant neurodegenerative disorders have been created using human BAC transgene approaches. These model mice successfully express human transgenes in human-like patterns and recapitulate disease-like phenotypes (Crook & Housman, 2011; Ferrante, 2009; Shenoy et al., 2022; Taguchi et al., 2019; Yang & Lu, 2008). Previously we constructed *Pkcd-BAC-Cre* transgenic mice and obtained independent lines with reproducible expression patterns as well (Zhang et al., 2016)(Supplementary Fig. 1).We therefore decided to use BAC approaches to create "volized" *Oxtr* mouse lines.

To create pv*Oxtr-P2A-Cre* BAC transgenic mouse line, the prairie vole BAC clone we used includes the entire pv*Oxtr* locus (the coding sequence and all the introns) with the full intergenic sequence upstream (150kb) and downstream of the pv*Oxtr* coding region (9kb) (Fig.1 B). The BAC clone contains a portion of *Rad18*, minus the first 11 exons, located upstream of pv*Oxtr*, and *Cav3*, minus the first exon including the start codon, downstream of pv*Oxtr*. Therefore, there will be no interference of these two flanking transgenes on behavior analysis, and the proximal topological structure around pv*Oxtr* locus is preserved to the maximum extent. A P2A-NLS-Cre cassette was inserted in-frame just before the *Oxtr* stop codon to ensure co-expression of *Cre* and *Oxtr* (Fig.1 C). Transgenic mice were generated by pronuclear injection using C57BL/6J zygotes. Proper integration of the reporter into the BAC clone was confirmed using gene specific PCR assays and sequencing (Fig.1 C, D and data not shown). We obtained 11 founder mice carrying the transgenes, which was verified by PCR with multiple primer sets (Fig.1 C, E). One founder line was sterile, and two founder lines did not show germ-line transmission. Eight founder lines successfully produced offspring and stably transmitted the transgene to at least 3 generations. We named these lines "Koi", meaning "love" in Japanese.

Each Koi line showed a unique expression pattern of transgene in brain, yet conserved expression in mammary gland

We systemically evaluated 8 Koi lines by crossing them with ROSA-26-NLS-*LacZ* mice, a Cre reporter mouse line expressing nuclear-localized beta-galactosidase (Kandasamy et al., 2021; Zhang et al., 2016). Since Lac-Z is only expressed in the nucleus of double positive (CRE+, LacZ+) cells, but not in the neuronal processes, we could easily assess the expression pattern of our transgene. We found that each Koi founder line displayed a unique pattern of expression in brain distinct from that of wildtype mice or prairie voles (Fig.2 A-O, and supplementary Fig.2). Almost all Koi lines showed transgene expression in olfactory bulb, lateral septum (Fig.2 F-I and Supplementary Fig.2 B,E,H,K) and ventromedial nucleus of the hypothalamus (Fig.2 K-N and Supplementary Fig.2 C,F,I,L), though with different intensities, suggesting that these regions constitute a stable core *Oxtr* expression network, as these regions also express OXTR in mice and voles (Inoue, Ford, Horie, & Young, 2022; Newmaster et al., 2020). Several Koi lines expressed the transgene in some brain regions specific for vole *Oxtr* expression, including nucleus accumbens (NAc) (Fig.2 A,B,D and Supplementary Fig.2 A,G,J), prefrontal cortex (PFC) (Fig.2 A,B,C and Supplementary Fig.2 J), lateral amygdala (Fig.2 K,L,M and Supplementary Fig.2 C,I,L) and deep layers of cingulate cortex (Fig.2A,B,C and Supplementary Fig.2 C,L), which suggested that cis regulatory elements in the BAC are capable of mediating the expression of *Oxtr* in the reward and reinforcement circuitry of brain, albeit depending on the sequence/structure of distal sequences >150 kb upstream and >21 kb downstream of the transcription start site. None of the Koi lines exactly "mirrored" the vole-specific expression patten. Six of the Koi lines expressed the transgene in broad areas of thalamus (Fig.2 K,L,N and Supplementary Fig.2 C,I,L), reminiscent of the strong expression of V1a vasopressin receptor (*Avpr1a*) in the thalamus (Larry J. Young & Zhang, 2021). Intriguingly, the expression of OXTR in mammary glands showed similar pattern among all the Koi lines and *mouseOxtr(mOxtr)-Ires-Cre* knock-in line (Fig.2 P-T and Supplementary Fig.3).

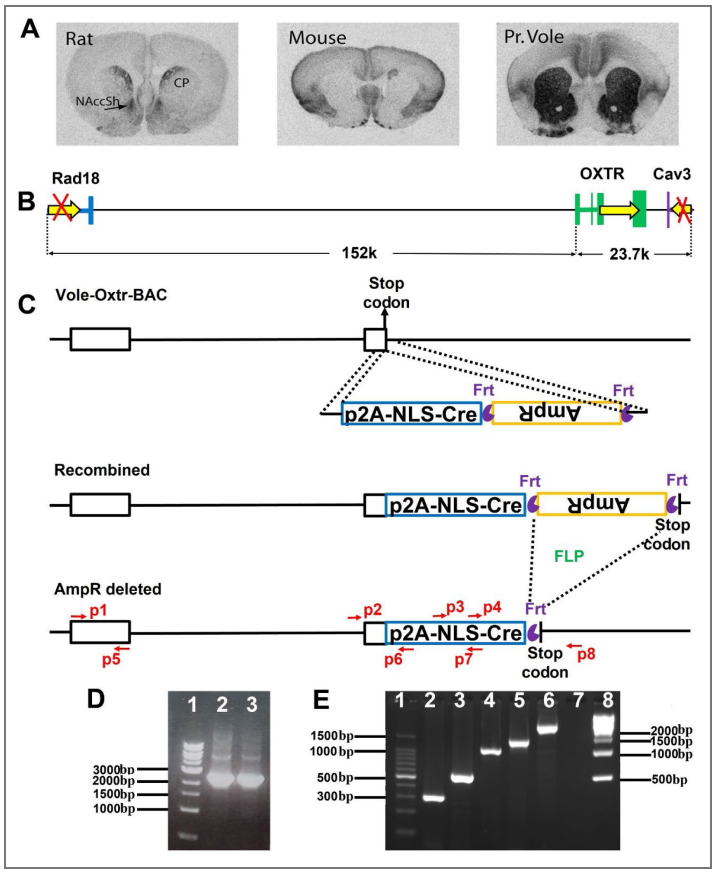

Fig. 1. Construction of Koi lines.

(A) Example of the remarkable species difference of brain OXTR distribution. OXTR receptor autoradiography in dorsal caudate putamen (CP) and nucleus accumbens shell (NAccSh) of rat, mouse, and prairie voleis (Adapted Froemke and Young(Froemke & Young, 2021)). (B) The pv*Oxtr* BAC clone contains the entire sequence of pv*Oxtr* gene (colored green), the complete intergenic sequence both upstream and downstream of pv*Oxtr* gene, the 12th exon of *Rad18* (colored blue) and the 2nd exon of *Cav3* (colored purple). The yellow arrows indicate the direction of transcription. (C) Schematic diagram of the strategy to generate Koi mice. The P2A-NLS-Cre-Frt-Amp-Frt cassette was inserted in-frame right before the stop codon of *Oxtr*. And the ampicillin selection marker was deleted by 706-Flpe. PCR primers for verifying the targeted alleles are shown as red arrows. (D) Two correctly modified vector clones were verified by using PCR with p2 and p8. (E) Koi lines were verified by 5 pairs of primers. From Lane1 to Lane8 are 100bp marker, p3+p7, p2+p6, p2+p7, p4+p8, p2+p8, blank and 1kb marker.

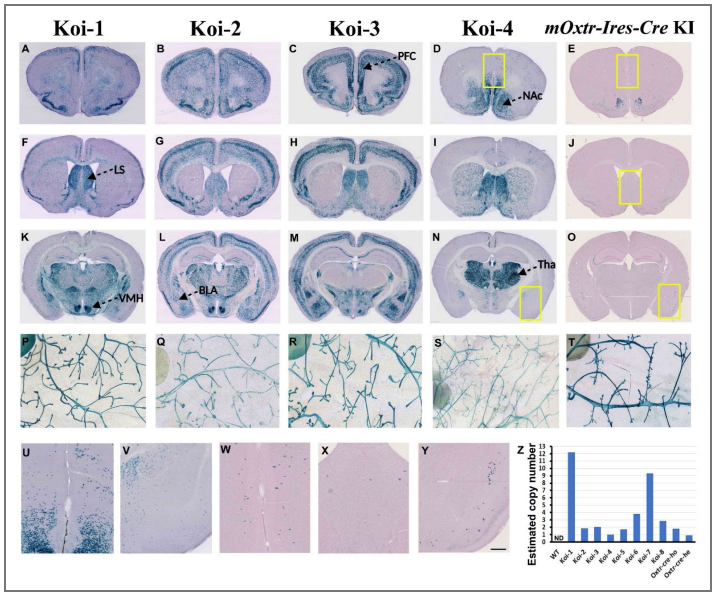

Fig. 2. Transgenic CRE mediated Lac-Z reporter gene expression in the brain and mammary gland of Koi lines.

X-gal staining of the brains and mammary glands are from the double positive (*Cre*+, *LacZ*+) offspring from Koi-1 (A, F, K, P), Koi-2 (B, G, L, Q), Koi-3 (G, H, M, R), Koi-4 (D, I, N, S) and *mOxtr-Ires-Cre* knock-in line (E, J, O, T). The *mOxtr-Ires-Cre* KI line used contains Cre (and an HA tag) inserted in the third exon, right after the start codon. Note that regardless of the insertion site of Cre in the mouse genome DNA or pvOxtr-BAC transgene, *Oxtr* expression visualized by Lac-Z staining in the mammary gland was comparable between the mOxtr-Ires-Cre KI and Koi lines. This contrasts with the diverse expression patterns of *Oxtr* expression in the brain. U, V, M, X, Y are the magnified images of the areas within the yellow-border squares from D, N, E, J, O, respectively, to show the distribution of low-density Lac-Z positive cells in these areas. Scale bar=1mm (A-O), 500um (P-T) and 200um (U-Y). (Z) The estimated copy number of transgene of all Koi lines. See Supplementary Figure 2 for images of Koi-5-8 lines. PFC=prefrontal cortex, LS=lateral septum, BLA=basolateral amygdala, VMH=ventromedial nucleus of the hypothalamus, Tha=thalamus.

Transgenes that are introduced by pronuclear injection typically integrate into a single site of the genome as tandem concatemers (Smirnov et al., 2019). BAC copy number variation and different insertional loci can lead to distinct patterns of ectopic expression, and increased BAC transgene copy numbers often correlate with increased BAC gene expression (S. Gong et al., 2007). We then examined the relationship between transgene copy number and LacZ signal using quantitative genomic PCR (Chandler et al., 2007). As expected, the copy number of WT, heterozygous and homozygous *mOxtr-Ires-Cre* knock-in mice was 0, 1 and 2 respectively (Figure.2 Z). The copy number of transgene in Koi lines are: Koi-1 (12), Koi-2 (2), Koi-3 (2), Koi-4 (1), Koi-5 (2), Koi-6 (4), Koi-7 (9), Koi-8 (3). Koi-6 and Koi-7 showed the most limited expression of reporter gene, though the copy number of transgene were 4 and 9 respectively. Koi-4 showed strong expression of reporter gene in NAc, septum and thalamus, though there was only 1 copy of transgene. Therefore, integration site rather than copy number is the reason of the variant BAC transgene expression patterns across our Koi lines.

Adult brain OXTR binding patterns differ across Koi lines

To detect the distribution of OXTR protein in adult Koi lines without the interference of endogenous mouse OXTR (mOXTR) signal, Koi lines were crossed with *mOxtr*$^{-/-}$ line twice sequentially to produce Koi: m*Oxtr*$^{-/-}$ mice, and pvOXTR binding was detected using receptor autoradiography. We focused on analyzing 4 lines: Koi-1: m*Oxtr*$^{-/-}$, Koi-2: m*Oxtr*$^{-/-}$, Koi-3: m*Oxtr*$^{-/-}$ and Koi-4: m*Oxtr*$^{-/-}$ based on the strong expression of reporter gene in behaviorally relevant neuronal populations. Autoradiography demonstrated functional pvOXTR in brain resembling to some extent Cre-induced reporter gene expression (Fig.3). Brain OXTR binding of Koi-3: m*Oxtr*$^{-/-}$ was consistent with Lac-Z expression in the reporter line (Fig.2 C, H, M and Fig.3 C, H, M). Interestingly, the OXTR binding in PFC of Koi-3: m*Oxtr*$^{-/-}$ was similar to that of prairie vole (Figure.3 C). In contrast, Koi-4: m*Oxtr*$^{-/-}$ showed low OXTR binding in NAc when compared with the high Lac-Z staining (Fig.2 D and Fig.3 D). Koi-2: m*Oxtr*$^{-/-}$, the line which displayed the expression of reporter genes in the broadest regions, did not show strong signal in autoradiography. It is interesting that Layer IV of cortex in Koi-4: m*Oxtr*$^{-/-}$ showed strong OXTR binding (Figure.3 I and N), which is highly likely to originate from the axon projections from the thalamus (Fig.2 N), as was previously reported for NAc projections in voles (Inoue et al., 2022). Consistent with Lac-Z expression, we do not see a clear relationship between OXTR binding and transgene copy number. For example, Koi-1: m*Oxtr*$^{-/-}$ showed rather low OXTR signal (Fig.3 A, F, K) with the highest copy number, while Koi-4: m*Oxtr*$^{-/-}$ showed very strong OXTR signal at lateral septum and thalamus (Fig.3 I, N), with the lowest copy number.

Oxtr mRNA level in Koi-3: m*Oxtr*$^{-/-}$ and Koi-4: m*Oxtr*$^{-/-}$ was further investigated with Fluorescent RNAscope *in situ* hybridization (Fig.4). Consistent with Lac-Z expression in the reporter line, Koi-3: m*Oxtr*$^{-/-}$ showed strong signal in PFC and Ctx (Fig.4 A, C), while Koi-4: m*Oxtr*$^{-/-}$ showed prominent signal in NAc and Thalamus (Fig.4 B, D). qRT-PCR analysis further revealed that adult Koi-4: m*Oxtr*$^{-/-}$ mice had the highest Oxtr mRNA signal in the ventral striatum, several fold higher than WT, consistent with the Lac-Z staining in the reporter line (Fig.5 A, B). The discrepancy of OXTR signal in NAc of Koi-4: m*Oxtr*$^{-/-}$ between autoradiography and Lac-Z staining/RNAscope/qRT-PCR may, therefore, be due to the translational regulation or differences in the sensitivity of the detecting methods.

Although none of our Koi lines mirrored the endogenous OXTR expression in prairie voles, we confirmed strong expression of pv*Oxtr* in olfactory bulb of Koi-1line, PFC and amygdala of Koi-3line, striatum and thalamus of Koi-4 lines, and the broad expression of pv*Oxtr* in Koi-2 line. As OXTR signaling in some of these regions are similar to that in voles, albeit in separate lines, and postulated to be involved in vole social behavior (H. Walum & L. J. Young, 2018), we used these lines to address the question of whether variation in *Oxtr* transcription in brain can lead to variation in social behaviors.

Fig. 3. The expression of OXTR in adult brain of Koi lines.

Autoradiographs illustrate the distribution of OXTR binding in adult Koi-1: m*Oxtr*$^{-/-}$ (A, F, K), Koi-2: m*Oxtr*$^{-/-}$ (B, G, L), Koi-3: m*Oxtr*$^{-/-}$ (C, H, M), Koi-4: m*Oxtr*$^{-/-}$ (D, I, N) and wild type (WT) (E, J, O). All Koi mice used for this analysis were pv*Oxtr-P2A-Cre*: m*Oxtr*$^{-/-}$ mice in which the pvOXTR was expressed while endogenous mOXTR was absent. PFC=prefrontal cortex, LS=lateral septum, BLA=basolateral amgydala, VMH=ventromedial nucleus of the hypothalamus, Tha=thalamus. Scale bar=1mm.

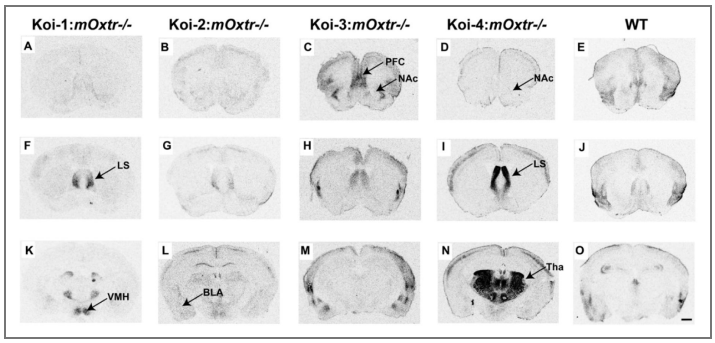

Fig. 4. mRNA expression of *Oxtr* in the adult brain of Koi lines.

Oxtr mRNA (red) was labeled with in situ hybridization against DAPI for nuclei labelling (purple). (A) and (C) show clear expression of *Oxtr* in the PFA and Ctx in Koi-3: m*Oxtr*$^{-/-}$. (B) and(D) show clear expression of *Oxtr* in the NAc and Tha in Koi-4: m*Oxtr*$^{-/-}$. All Koi mice used for this analysis were pv*Oxtr-P2A-Cre*: m*Oxtr*$^{-/-}$ mice, in which the pvOXTR was expressed while endogenous mOXTR was absent. PFC=prefrontal cortex, NAc= Nucleus accumbens, Ctx=Cortex, Tha=thalamus. Scale bar=400um for A and B, 500um for C and D.

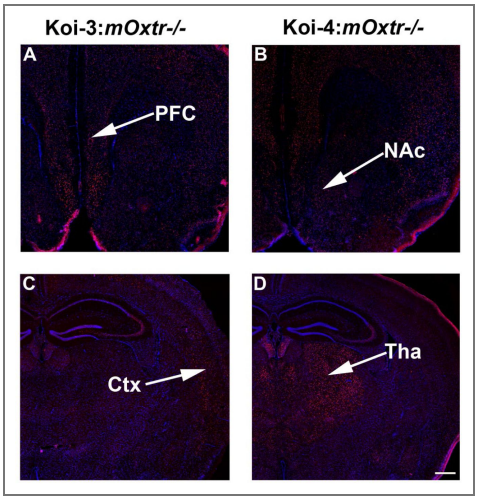

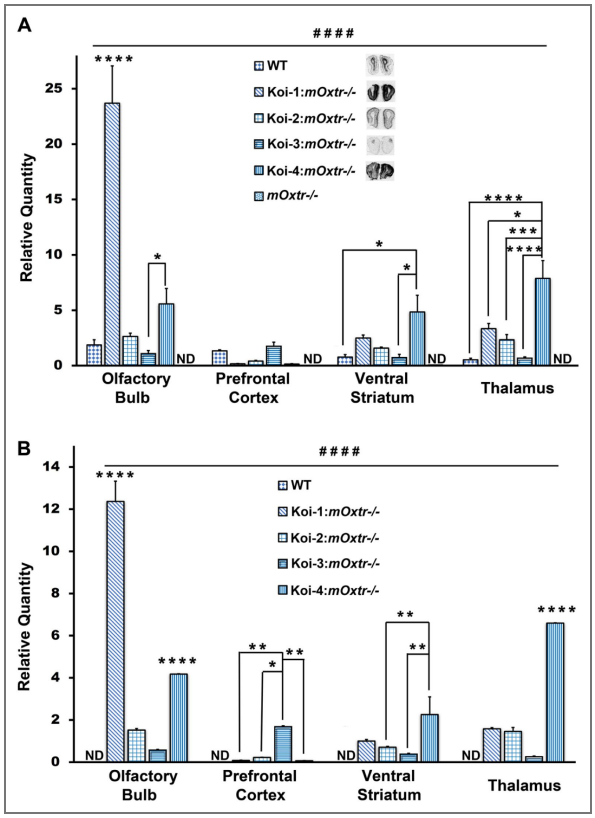

Fig. 5. Quantitative PCR analysis of *Oxtr* mRNA expression in different brain regions of Koi lines.

(A) A primer set recognizing both m*Oxtr* and pv*Oxtr* was used to analyze *Oxtr* mRNA in olfactory bulb, prefrontal cortex, ventral striatum and thalamus from WT, Koi-1: m$Oxtr^{-/-}$, Koi-2: m$Oxtr^{-/-}$, Koi-3: m$Oxtr^{-/-}$, Koi-4: m$Oxtr^{-/-}$ and $mOxtr^{-/-}$ mutant mice, n=4 for each genotype. Note that the level of *Oxtr* mRNA in $mOxtr^{-/-}$ mutant mice was nondetectable (ND). The autoradiograph of OXTR binding in olfactory bulb from each line were shown alongside the legend. There was a significant interaction between position and genotype F (12,64) =26.33, p<0.0001; Post hoc Bonferroni test revealed that *Oxtr* expression level in olfactory bulb of Koi-1: m$Oxtr^{-/-}$ was significantly higher than that of other genotype groups (p<0.0001 for all), and that of Koi-4: m$Oxtr^{-/-}$ was significantly higher than that of Koi-3: m$Oxtr^{-/-}$ p<0.05. And the striatum of Koi-4: m$Oxtr^{-/-}$ expressed significantly higher *Oxtr* when compared with WT and Koi-3: m$Oxtr^{-/-}$ (p<0.05 for both). The *Oxtr* expression level in thalamus of Koi-4: m$Oxtr^{-/-}$ was significantly higher than other genotype groups (p<0.0001 when compared with WT and Koi-3: m$Oxtr^{-/-}$, p<0.001 when compared with Koi-2: m$Oxtr^{-/-}$, p<0.05 when compared with Koi-1: m$Oxtr^{-/-}$) (B) A primer set specifically recognizing pv*Oxtr.* was used to analyze *Oxtr* mRNA in WT, Koi-1: m$Oxtr^{-/-}$, Koi-2: m$Oxtr^{-/-}$, Koi-3: m$Oxtr^{-/-}$ and Koi-4: m$Oxtr^{-/-}$ mic, n=4 for each genotype. Note that the level of *Oxtr* mRNA in WT mice was barely detectable. There was a significant interaction between position and genotype F (9,48) =89.25, p<0.0001; Post Hoc Bonferroni test revealed that *Oxtr* expression level in the olfactory bulb of Koi-1: m$Oxtr^{-/-}$ was significantly higher than that of other genotype groups (p<0.0001 for all), and that of Koi-4: m$Oxtr^{-/-}$ was significantly higher than that of Koi-2: m$Oxtr^{-/-}$ and Koi-3: m$Oxtr^{-/-}$ (p<0.0001 for both). The *Oxtr* expression level in prefrontal cortex of Koi-3: m$Oxtr^{-/-}$ was significantly higher than that of other groups (p<0.01 when comparing with Koi-1: m$Oxtr^{-/-}$ and Koi-4: m$Oxtr^{-/-}$; p<0.05 when comparing with Koi-2: m$Oxtr^{-/-}$). And the striatum of Koi-4: m$Oxtr^{-/-}$ expressed significantly higher *Oxtr* when comparing with Koi-2: m$Oxtr^{-/-}$ and Koi-3: m$Oxtr^{-/-}$ (p<0.01 for both). The *Oxtr* expression level in thalamus of Koi-4: m$Oxtr^{-/-}$ was significantly higher than that of other genotype groups (p<0.0001 for all). All Koi mice used for this analysis were pv*Oxtr-P2A-Cre*: m$Oxtr^{-/-}$ mice, in which the pvOXTR was expressed while endogenous mOXTR was absent. The significance of interaction between genotype and brain region: # # # # p<0.0001. The significance of single main effect of genotype:*p<0.05; **p<0.01; ***p<0.001; ****p<0.0001.

Different Koi lines showed diverse behaviors in a Partner Preference Test

The partner preference test is widely used as a laboratory proxy for pair bonding in prairie voles. In a pilot study, we found that Kio-4 female mice on a m*Oxt*$^{+/+}$ background showed a preference for their mate relative to a novel male. We then focused on the females of 4 lines (Koi-1, 2, 3, 4) based on transgene expression in PFC, BLA or NAc. Again, we bred the Koi lines with *mOxtr*$^{-/-}$ mice (both on C57/B6 background) to generate Koi: m*Oxtr*$^{-/-}$ offspring expressing only pv*Oxtr*. Partner preference tests (PPT) were performed in ovariectomized females after 21 days of cohabitation with 3 mating bouts elicited by estrogen and progesterone injections on days 2, 9 and 16. We divided our analysis into 3 phases (Fig.6 A, B). In the habituation phase, the experimental subject was habituated to the chamber for 5 minutes with both pen-boxes empty. In the recognition phase, the partner stimulus animal was restricted in one pen-box, and a novel "stranger" male was restricted in another pen-box, and the experimental female was allowed to explore the arena for 10 minutes to test social novelty preference. In the preference phase, the positions of the partner stimulus animal and the "stranger" stimulus animal were switched to avoid position bias, and the female was allowed to explore the chamber for an additional 20 minutes.

Mixed ANOVA was conducted to examine the effect of genotype and the stimulus box on the area stay time during all the phases. In the habituation phase (Fig.6 C), there was no statistically significant interaction between the effects of genotype and position of empty pen-box on stay time, $F(4, 60) = 0.69$, $p = 0.6$. There was no difference in position preference for all the groups, $F(1,60) = 0.03$, $p = 0.87$. In the recognition phase (Fig.6 D), there was a main effect of stimulus animal (i.e., partner or stranger) on stay time, the time staying in close proximity to the partner was significantly shorter than the time stay with stranger animal ($F(1,60) = 15.38$, $p = 0.0003$). There was a main effect of genotype on social stay time, $F(4,60) = 2.62$, $p = 0.04$, and a significant interaction between the effects of genotype and stimulus animal on area stay time, $F(4, 60) = 2.61$, $p = 0.04$. Bonferroni adjusted pairwise comparisons were applied to analyze the simple main effects. Koi-4: m*Oxtr*$^{-/-}$ and WT mice spent significantly longer time in "stranger" area than in "partner" area ($p = 0.0001$ for Koi-4: m*Oxtr*$^{-/-}$; $p = 0.028$ for WT), demonstrating a typical novelty preference. There was no significant difference between the stay time with "stranger" and "partner" for Koi-1: m*Oxtr*$^{-/-}$ ($p = 0.96$), Koi-2: m*Oxtr*$^{-/-}$ ($p = 0.49$) and Koi-3: m*Oxtr*$^{-/-}$ ($p = 0.09$) mice. In the preference phase (Fig.6 E), conducted after both stimulus mice were presumably familiar following the initial 10 min recognition phase, there was no main effect of stimulus animal on stay time, $F(1,60) = 0.04$, $p = 0.84$. There was no main effect of genotype on stay time either, $F(4,60) = 1.36$, $p = 0.26$. There was a statistically significant interaction between the effects of genotype and stimulus animal on area stay time, $F(4, 60) = 4.64$, $p = 0.003$. Bonferroni adjusted pairwise comparisons revealed that Koi-2: m*Oxtr*$^{-/-}$ mice spent significantly longer time in "stranger" area than in "partner" area ($p = 0.024$). In contrast, Koi-4: m*Oxtr*$^{-/-}$ mice spent significantly longer time in "partner" area than in "stranger" area ($p = 0.002$). There was no significant difference between the stay time with "stranger" and "partner" for WT ($p = 0.99$), Koi-1: m*Oxtr*$^{-/-}$ $p = 0.16$) or Koi-3: m*Oxtr*$^{-/-}$ ($p = 0.45$) mice.

Different Koi lines showed diverse behaviors in Pup Retrieval Test

Based on the abundant pvOXTR of Koi-3and Koi-4 in reward-related brain regions (Fig.3 C,D,H,I,M,N), and the role of OXTR in mediated maternal care in mice and voles (Carcea et al., 2021; Marlin, Mitre, D'Amour J, Chao, & Froemke, 2015; Olazábal & Young, 2006), we further tested the parental behaviors of these two lines in virgins (Fig.6 F, G). Mixed ANOVA was conducted to examine the effect of genotype and pup number (1-3) on the latency of pup retrieval. Mauchly's test showed that the sphericity was violated. Therefore, the Greenhouse-Geisser correction was used for the repeated measures ANOVA. There was a significant main effect of genotype on latency to retrieve, $F(2,48) = 29.58$, $p < 0.0001$. Koi-4: m*Oxtr*$^{-/-}$ took a significantly longer time to retrieve all the pups than WT and Koi-3: m*Oxtr*$^{-/-}$ ($p < 0.0001$ for both). There was also a significant interaction between the effects of genotype and retrieved pup number on the retrieval

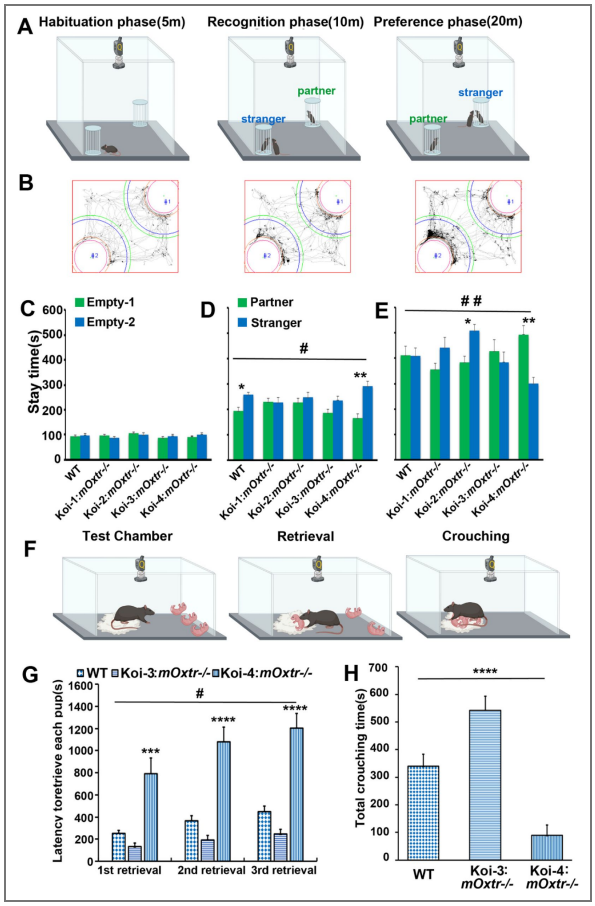

Fig. 6. Social behaviors of Koi lines.

(A) Illustration of the partner preference test (PPT) paradigm. The experimental mouse was placed in a chamber with an automatic monitoring system, where it could freely explore two pen-boxes localized in two diagonal corners. Habituation phase: two pen-boxes are empty. Recognition phase: a stimulating partner mouse is placed into one pen-box and a stimulating stranger mouse is placed in the other one. Preference phase: The positions of two stimulating mice are switched. (B) Representative traces of one experimental mouse during the three phases. (C-E) The stay time in the surrounding area of each pen box during three phases;(C) Habituation phase;(D) Recognition phase; (E) Preference phase. Samples sizes for the PPT are wild type(WT) (n=12), Koi-1: m*Oxtr*$^{-/-}$ (n=14), Koi-2: m*Oxtr*$^{-/-}$ (n=13) Koi-3: m*Oxtr*$^{-/-}$ (n=12) Koi-4: m*Oxtr*$^{-/-}$ (n=14). All the experimental mice are female. (F) The illustration of the procedure of the maternal behavior test. (G) Pup retrieval latency and (H) crouching time were recorded and analyzed. Sample sizes for the maternal behavior tests are WT (n=15), Koi-3: m*Oxtr*$^{-/-}$ (n=18), Koi-4: m*Oxtr*$^{-/-}$ (n=18). Significance of interaction between independent factors: # p<0.05; # # p<0.01. Significance of main effect or single main effect of genotype:*p<0.05; **p<0.01; ***p<0.001; **** p<0.0001. All Koi mice used for this analysis were pv*Oxtr-P2A-Cre*: m*Oxtr*$^{-/-}$ mice in which the pvOXTR was expressed while endogenous mOXTR was absent.

latency, F (2.40, 57.49) = 4.45, p =0.011. Post Hoc multiple comparisons with Bonferroni correction revealed that Koi-4: m*Oxtr*$^{-/-}$ took a significantly longer time to accomplish the 1st retrieval (p=0.0003 and p=0.0005), the 2nd retrieval (p<0.0001), and the 3rd retrieval (p<0.0001) when compare to WT and Koi-3: m*Oxtr*$^{-/-}$. And Koi-3: m*Oxtr*$^{-/-}$ took a significantly shorter time to accomplish the 1st retrieval (p=0.01), the 2nd retrieval (p=0.006), and the 3rd retrieval (p=0.003) when compare to WT.

Crouching time was analyzed as well (Fig.6 F, H). There was a statistically significant difference between groups as determined by one-way ANOVA (F (2,48) = 27.56, p <0.0001). A Bonferroni post hoc test revealed that the crouching time of Koi-3: m*Oxtr*$^{-/-}$ was statistically significantly longer than WT (p=0.008) and Koi-4: m*Oxtr*$^{-/-}$ (p<0.0001). Additionally, the crouching time of Koi-4: m*Oxtr*$^{-/-}$ was statistically significantly shorter than WT (p=0.001). Therefore, two Koi lines with different OXTR expression pattern demonstrated quantitative differences in parental behavior tests.

The TAD structure of brain *Oxtr* is markedly distinct from that of both *Oxt* and peripheral *Oxtr*

The divergent brain expression patterns across our Koi lines suggest that distal elements external to our BAC cassette contribute to the variation in *Oxtr* expression. TADs represent a key feature of hierarchical genome organization comprising regions of high chromatin inter-connectivity, and TAD formation appears to be linked to transcription regulation (Beagan & Phillips-Cremins, 2020; Dekker, Rippe, Dekker, & Kleckner, 2002; Dixon et al., 2012; Rajderkar et al., 2023). TADs are generally conserved within the same tissue type across different species. We therefore utilized publicly available 3D chromatin datasets from mouse (Extended data Table7-1) and analyzed the TAD structure of *Oxtr* and *Oxt*, both in brain related tissues/cells and peripheral tissues/cells. We discovered that *Oxtr* is consistently located at the boundary region of TAD structures across several tissues and cell lines (Fig.7 A). Specifically, only in brain related samples (whole brain tissue, neural progenitor cells, and cortex tissue), *Oxtr* is situated at the boundary of a large inter-TAD interaction between two neighboring TADs (Fig.7 A). In contrast, the oxytocin peptide gene, *Oxt*, which is expressed in a highly conserved brain pattern across vertebrates, lacks organized TAD structures (Fig.7 B). These findings demonstrate that the TAD landscape differ dramatically between *Oxtr* and *Oxt*, and highlight that the 3D genomic architecture surrounding the *Oxtr* gene varies between brain tissues/cells and peripheral tissue/cells. There exists clear long-distance interaction in brain *Oxtr* gene TAD structure. The presence of extensive long-distance chromatin interactions around *Oxtr* in brain tissues may at least partially explain why its expression is hypersensitive to distal regulatory sequences beyond the range of a BAC construct. Moreover, such large inter-TAD interactions likely expose *Oxtr* regulation to a broader set of cis- and trans-acting influences, rendering brain *Oxtr* expression inherently more variable across individuals and species.

Discussion

Diversity of *Oxtr* expression patterns causes diversity of social behaviors

The diverse OXTR expression of our Koi lines is reminiscent of the diverse OXTR expression across different species. The unique expression pattern of *Oxtr* in monogamous prairie vole was mainly observed in PFC, NAc and BLA. We obtained expression in all of these specific regions, but in 3 separate lines. These Koi lines with distinct brain OXTR expression pattern provided an opportunity to test the effect of variation of OXTR expression on diverse social behaviors.

It is intriguing that Koi-4 line showed preference to their mating partners but not strangers, which is a behavior specific in prairie voles but not in mice. Multiple studies suggested that NAc and PFC play important roles in mediating partner preference behavior in prairie voles (Amadei et al., 2017; Hasse Walum & Larry J. Young, 2018). Consistently, the Koi-4 line showed robust

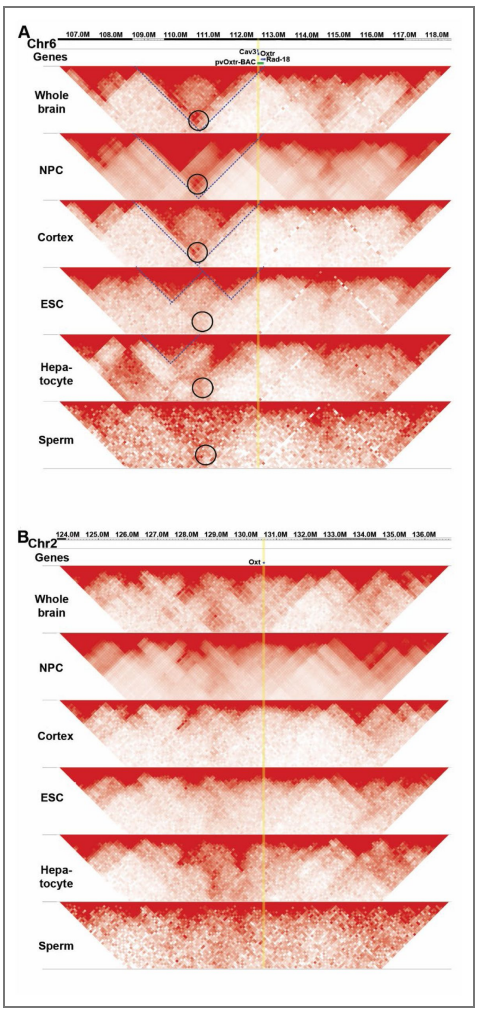

Fig. 7. Heatmap of the chromatin contacts surrounding *Oxtr* and *Oxt* across mouse tissues/cells from megabase-size visualization.

(A) Heatmap of the chromatin contacts surrounding *Oxtr* across mouse tissues/cells: *Oxtr* is located at a TAD boundary region. The increase of interactions characterizes the TADs structure and the interaction of two neighboring TADs can be more clearly observed in brain-related samples. Blue dashed lines were prepared to help observing the TAD structures, and black circles were prepared to help observing the long-distance interaction obtained from Hi-C interaction matrices surrounding *Oxtr*. (B) Heatmap of the chromatin contacts surrounding *Oxt* across mouse tissues/cells. No TAD structure was observed surrounding *Oxt* locus.

transgene expression in these brain regions. Notably Koi-4 line also demonstrated strong *Oxtr* expression in the entire thalamus region, which reminds us the distribution of *Avpr1a* (Phelps & Young, 2003). Given the fact that OXTR and AVPR1A genes were derived from a duplication of a single ancestral gene (Grinevich, Knobloch-Bollmann, Eliava, Busnelli, & Chini, 2016), it is not surprising that the similar expression regulation machinery exists. Recent studies indeed revealed the critical functions of different thalamic nuclei in social memory and cognition (Chen et al., 2024; Kappel et al., 2022; Rangel, Baldo, & Canteras, 2018; Wolff & Vann, 2019). Partner preference formation and maintenance needs to recruit multi- and cross-modality sensation, social recognition and social memory, selective attention, arousal, and reward systems. We propose a model that the sufficient upregulation of the OXTR expression in one or multiple of these systems can tune the network and boost partner preference behavior. In addition, the maternal behavior in Koi-3 and Koi-4 lines was enhanced and reduced, respectively. This result suggested that OXTR signaling facilitates social partner preference and maternal care by coordinating activity across different neural networks. A main conclusion of our study is that simply by redistributing OXTR binding in space, variation in social preference and parental behaviors emerged, which conceivably could impart advantageous behaviors that natural selection could act upon and amplify. Future study will determine how the variation in OXTR distribution in our Koi lines affects neural circuits mediating social behaviors.

A potential genetic mechanism contributing to diversity of brain OXTR expression

The sex steroid and oxytocin systems play important roles in modulating reproductive and related social behaviors in vertebrates. Sexual behavior, e.g., the motivation to mate and motor patterns, is highly conserved across vertebrate species. By contrast, social behaviors, e.g., sociality, mating strategy (monogamy vs polygamy), parental and alloparental behaviors are more nuanced and can vary dramatically across species in the same genus or even between individuals of a single species. It is interesting, therefore, that the distribution of steroid receptors is quite conserved among species (L. J. Young & Crews, 1995), while that of the OXTR is extremely diverse across and even within species (Froemke & Young, 2021; Larry J. Young & Zhang, 2021). It is even more interesting that although the distribution of OXTR is diverse, its ligand, oxytocin, is expressed in a highly conserved neuroanatomical pattern in vertebrates (Ross & Young, 2009). Previous work showed that three independent rat lines with puffer fish oxytocin BAC transgene (containing 16 kb of 5' flanking regulatory sequence) expressed the *Fugu* oxytocin transcript specifically in oxytocin neurons in rat (Venkatesh, Si-Hoe, Murphy, & Brenner, 1997). Moreover, a similar transgenic experiment transferring approximately 5 kb of the *Fugu* oxytocin already resulted in a faithful expression of the fish genes in mouse oxytocin neurons (Gilligan, Brenner, & Venkatesh, 2003). These studies suggest there is a remarkably conserved transcriptional regulatory machinery across species, even between the *Fugu* and rodent oxytocin genes, despite being separated by 400 million years of evolution.

The GENSAT (Gene Expression Nervous System Atlas) Project demonstrated that most BAC transgenes reliably recapitulate endogenous expression across independent lines, provided that extensive flanking intergenic regions are included (Gerfen et al., 2013; S. Gong et al., 2007; Shiaoching Gong et al., 2003; Heintz, 2004; Schmidt et al., 2013). Our pv*Oxtr* clone contained the entire locus with full upstream and downstream intergenic sequences, yet the transgenic lines we generated displayed strikingly divergent brain expression patterns. These differences were not explained by transgene copy number, but instead reflected strong insertion-site effects. This paradox contrasts with the general reproducibility of BAC transgenics and echoes the observation that virtually every rodent or primate species has a unique distribution of OXTR binding in the brain.

The 3D genomic structure analysis showed that the *Oxtr* loci sit within large TAD structures, increasing its exposure to distal regulatory elements through an expanded interaction landscape, whereas *Oxt* lacks organized TAD structures. This difference might explain why short promoter sequences suffice for conserved *Oxt* expression across species, while even a large BAC is

insufficient for precise, reproducible transcription regulation of *Oxtr*. The large TAD and extensive long-range interactions render *Oxtr* especially sensitive to chromosomal context, accounting for the position effects we observed.

It is also noteworthy that pv*Oxtr* expression in mammary gland (which is responsible for essential lactation in mammals) was conserved across all Koi lines, indicating that the essential cis-regulatory elements for peripheral expression are captured within the BAC and are resistant to position effects. This conclusion is consistent with the chromatin architecture we observed: the chromatin landscape differs considerably between brain-related tissues and peripheral tissues. There exists an obvious increase of long-distance interactions between neighboring TADs, forming a larger TAD structure in brain-related tissues but not peripheral tissues. Moreover, critical peripheral regulatory sequences may be clustered proximally around the locus, so that they fall entirely within the BAC. By comparison, in brain tissues, regulatory elements are dispersed across a much broader genomic interval, extending beyond the BAC. Together, the larger interaction landscape and distributed regulatory architecture in brain tissues likely explain why BAC constructs are sufficient for peripheral but not brain expression of *Oxtr*.

This is well aligned with broader principles of genome organization: subtle changes within 3D chromatin structure may result in substantial changes in local gene expression (Xiao, Hafner, & Boettiger, 2021). TADs also display increased SNPs and structure variations (SVs) density and higher recombination rate compared to inter-TAD regions(Beagan & Phillips-Cremins, 2020; Dekker et al., 2002; Dixon et al., 2012; Rajderkar et al., 2023). In fact, SNPs in the *Oxtr* intron explains 74% of the variance in striatal *Oxtr* expression and social attachment in prairie voles (King et al., 2016) and it is possible that these SNPs near *Oxtr* are linked to variations of long-range chromosomal interaction. Collectively, these evidences support the notion that brain *Oxtr* expression is hyper-sensitive to genetic variation.

Such an organization may endow *Oxtr* with enhanced evolvability. Oxytocin is a secreted neuromodulator that can diffuse along axons and through the extracellular space(Leng & Ludwig, 2008; Mitre et al., 2016; Parmaksiz & Kim, 2025). Its functional effects depend critically on the precise localization of its receptors, as the spatial distribution of oxytocin receptors determines the neural circuits engaged and the behavioral outcomes elicited. By making brain expression more reliant on distal regulatory sequences, *Oxtr* becomes subject to a wider range of cis- and trans-acting influences, rendering its expression in the brain inherently more variable across individuals and species. This variability allows oxytocin signaling to recruit novel neural circuits and modulate diverse aspects of social behavior, thereby contributing to the evolutionary diversification of sociality. Future studies should aim to resolve the precise mechanisms underlying this variability—for example, by identifying which distal regulatory elements physically interact with *Oxtr* within brain-specific chromatin architectures.

Ideas and Speculation

In summary, our results revealed that region-specific expression of *Oxtr* in the brain requires long-distance interactions between proximal and distal cis-regulatory elements. In contrast, many other genes remained consistent across BAC-transgenic lines, indicating that proximal regulatory sequences within the BAC were sufficient to drive faithful expression in these tissues, and that this expression was resistant to positional effects.

Our findings support a broader hypothesis: genes vary in their regulatory robustness and evolutionary flexibility. We propose a framework dividing genes into two broad classes based on their transcriptional architecture—rigid and flexible genes. Rigid genes— perhaps comprising the majority of the genome—maintain core life-sustaining functions (e.g., metabolism, motor function, development, reproduction) and are typically regulated by compact proximal elements. Their expression is stable across species, and across individuals within a same species. For such genes, BAC constructs often recapitulate endogenous expression reliably—examples include CamKII, Protein Kinase C Delta(Pkcd), and other genes characterized in large-scale projects like GENSAT.

In contrast, a subset of genes are flexible genes—such as neuromodulatory receptors like *Oxtr* and potentially *Avpr1a* and *Drd4 (Dopamine receptor D4)*— possess inherently more fragile or flexible transcriptional regulation. Their expression is highly sensitive to multiple factors including the chromatin landscape and complex long-range regulatory interactions. We hypothesize that this regulatory sensitivity is not a flaw but an evolutionary feature—what we term transcriptional evolvability. Subtle genetic or epigenetic changes, such as SNPs, structural variants, or chromosomal rearrangements, may lead to variation in neuromodulator receptor expression, thereby altering the modulation of preexisting neural circuits. Such changes could unmask cryptic behavioral phenotypes or give rise to novel social traits without requiring changes to core neural architecture. For example, caregiving circuits might evolve into pair bonding, empathy, or romantic attachment, while defensive or aggressive circuits might become recontextualized into behaviors like jealousy or mate guarding.

This model of transcriptional evolvability helps explain why *Oxtr* and *Avpr1a* expression varies so markedly across and within species, while their ligands (*Oxt* and *Avp*) remain stably expressed. The functional consequence of receptor variability is amplified by the secreted and diffusive nature of these neuromodulators: even small shifts in receptor localization can profoundly alter which neural circuits are engaged and which behaviors are modulated. It also raises the possibility that the capacity for behavioral innovation is, at least in part, encoded in the regulatory fragility of a small set of genes. Our model carries profound implications. It suggests that the evolution of complex social behavior is driven not only by neural circuitry or protein function, but by the regulatory architecture of a small set of flexible genes. These genes serve as behavioral tuning knobs—sensitive to the chromosomal environment, and capable of generating diverse phenotypes in response to evolutionary or environmental pressures. This model also offers insight into variability in human social phenotypes, including those observed in psychiatric conditions such as autism or social anxiety disorders, where subtle changes in receptor gene regulation may lead to major phenotypic shifts. Further research into the regulatory logic of *Oxtr*, *Avpr1a*, and similar genes may reveal a generalizable mechanism by which genome structure enables behavioral diversity and adaptation across the animal kingdom.

Materials and Methods

pvOxtr-P2A-Cre BAC vector construction

The vole BAC clone (GeneBank: DP001214.1) containing the *Oxtr* locus was obtained from a prairie vole BAC library (CHORI-232) (Lisa A. McGraw et al., 2010; L. A. McGraw, Davis, Thomas, Young, & Thomas, 2012). The NLS (nuclear localization signal)-Cre-Frt-Amp-Frt cassette was obtained from Dr. Takuji Iwasato, and was slightly modified to introduce a P2A sequence (Kim et al., 2011). The P2A sequence was introduced using PCR with the following primers:

fw5'-ATGGGAAGCGGAGCTACTAACTTCAGCCTGCTGAAGCAGGCTGGAGA

CGTGGAGGAGAACCCTGGACCTCTCGAAACTGACAGGAGAACCACC-3';

rv5'-AGACTGGAGTCCGCATAGCCCCCCTCCCCCGCCCCAGGCGCGGTGGGCC

AGGCAGGTGGCTCACCTTGACCAAGTTGCTGAAGTTCCTATTCC-3'. The P2A sequence is underlined. And the resulting amplified cassette had the P2A upstream of the NLS-Cre. Then the P2A-NLS-Cre-Frt-Amp-Frt cassette was inserted in-frame right before the stop codon of Oxtr in the BAC clone using the Red/ET Recombineering kit (Gene Bridges GmbH, Heidelberg Germany) after adding homologous arms by PCR with the following primers: fw5'-CACCTTCGTCCTGAGTCGCCGCAGCTCCA GCCAGAGGAGCTG

CTCTCAACCATCTTCAGCAATGGGAAGCGGAGCTACTAAC-3';

rv5'-GAGGAGAGGGATACACACCAATAGGCACCTTATACAACTCCACGCAC

GGCCACCAGGGGCAGACTGGAGTCCGCATAGCC-3'. The ampicillin selection marker was deleted with the 706-Flpe-induced recombination method (Gene Bridges Heidelberg Germany). A correctly modified BAC clone was verified by using PCR at both the 5' and 3' junctions of the targeted

insertion with the following primer pair: fr5'-GCCTTCATCATCGCCATGCTCTT-3'(p2) and rv5'-GATGG CTGAGTG ACTGGCATCT-3'(p8);

The construct was further verified by sequencing using the following 7 primers specific either for BAC vector or the p2A-NLS-Cre fragment:

5'-CCTGCAGCCAACTGGAGCTTC-3'(p1); 5'-CTTCCTTGGGCGCATTGACGTC-3'(p5);

5'-TACCTGTTTTGCCGGGTCAG-3(p4); 5'-GCCTTCATCATCGCCATGCTCTT-3'(p2);

5'-CTGACCCGGCAAAACAGGTA-3'(p7); 5'-TCCGGTTATTCAACTTGCACCATGC-3'(p6);

5'-GATGGCTGAGTGACTGGCATCT-3'(p8).

Animals

pv*Oxtr-P2A-Cre* BAC transgenic mouse lines (Koi lines)

pv*Oxtr-P2A-Cre* BAC vector was digested with NotI for linearization and to remove the pTARBAC vector backbone. The *Vole-Oxtr-P2A-Cre* BAC linearized fragment was purified using CL-4B sepharose (Sigma-Aldrich), and injected into pronuclei of C57BL/6J zygotes. Mice carrying the BAC transgene were identified and confirmed using PCR with 5 pairs of primers: fr5'-TCGACCAGGTTCG TTCACTC-3'(p3) + p7; p2+ p6; p2 +p7; p4 +p8; p2+p8. 8 lines (Koi-1∼Koi-8) were confirmed with successful transgene inheritance. These lines were maintained on a congenic C57BL/6J background by backcrossing with wildtype C57BL/6J for assessments of BAC DNA copy numbers and initial transgene expression analysis. The ***ROSA-26-NLS-LacZ* mouse** line (Zhang et al., 2016) was obtained from Itohara Lab at RIKEN.

The ***mOxtr-Ires-Cre* knock-in** (Hidema et al., 2016) and ***mOxtr*$^{-/-}$ mutant** (Takayanagi et al., 2005) lines were obtained from Dr. Katsuhiko Nishimori at Tohoku University, and both were backcrossed with C57BL/6J for more than 10 generations. Each Koi line and *mOxtr-Ires-Cre* knock-in mice were crossed with *ROSA-26-NLS-LacZ* mice to generate Cre^{+}, LacZ^{+} double positive mice for further gene expression analysis. Female Koi mice were crossed with male m*Oxtr*$^{-/-}$ to produce offspring with the genotype of pv*Oxtr-P2A-Cre*(Koi): m*Oxtr*$^{+/-}$. These offspring were then bred to produce Koi: m*Oxtr*$^{-/-}$ mice expressing pv*Oxtr* while lacking endogenous *mOxtr*, and these mice were used for autoradiography, qRT-PCR and behavioral tests. All mice were generated using continuously housed breeder pairs and P21 as the standard weaning date. All the animal procedures were approved by University of Tsukuba Animal Care and Use Committee. Mice were housed under constant temperature and light condition (12 h light and 12 h dark cycle), and received food and water ad libitum.

Determination of transgene copy number

Custom Taqman® MGB probes were synthesized by oligoJp (Thermo Fisher, Japan) for detecting the transgenic *Cre* and the mouse *Jun* gene (internal control). The following primer pairs and probes were used: for the *Cre* assay, fr5'-ATGACTGGGCACAACAGACAAT-3'; rv5'-CGCTGACAGCCGGA ACAC-3'; probe: 5'-FAM-AAACATGCTTCATCGTCGGTC CGG-MGB-3'; for *Jun* assay, fr5'-GAGTGCTAGCG GAGTCTTAACC-3'; rv5'-CTCCAGACGGCAGTGCTT-3'; probe:

5'-VIC-CTGAGCCCTCCTCCCC-MGB-3'. Real-time PCR was performed using an Applied Biosystem7500. Transgene copy number was determined through absolute quantification (standard curve method) following the protocol described in (Chandler et al., 2007). Briefly, 2 microliters (20 ng) of genomic DNA samples or copy number standards were analyzed in a 20μL reaction volume with two primer-probe sets (*Cre*, *Jun*). The data from transgenic samples were then compared to a standard curve of calibrator samples that are generated by diluting purified BAC DNA (linearized) over a range of known concentrations into wild-type mouse genomic DNA. In addition, no-template controls were included in each experiment. All reactions were performed in triplicate.

Histology

Adult mice (3-4month old), 4 male and 4 female from each line/generation were analyzed for 3 generations. Mice were perfused intracardially with 4% formalin in 0.1M sodium phosphate buffer. Brains were embedded in 2% agarose in 0.1M PB and cut into 100-m-thick sections with a Micro-slicer (Dosaka, Kyoto, Japan). Mammary glands were isolated from virgin female mice (2month old), 2 mice/each line were analyzed. The brain slices and whole mount mammary glands preparation were stained in X-gal solution (5 mM K3FeCN6, 5mMK4FeCN6,2mMMgCl2, 0.02% NP-40, 0.01% Na-deoxycholate, 1 mg/ml X-gal in 0.1M PB) at 37°C for 6 hours and then were stained with hematoxylin.

All experiments were done with positive and negative controls (Cre^+, $LacZ^-$) to monitor the reliability of the X-gal staining. Images were caught by Nanozoomer 2.0-HT slide scanner (Hamamatsu Photonics).

Receptor Autoradiography

OXTR autoradiography was performed as previously described (Inoue et al., 2022). Briefly, freshly frozen brains were stored at -80°C. Coronal sections were cut in a cryostat and 20 µm sections were collected and then stored at -80°C until use in autoradiography. Brain sections were removed from -80°C storage and air dried, and then fixed for two minutes with 0.1% paraformaldehyde in PBS at room temperature, and rinsed twice in 50 mM Tris buffer, pH 7.4, to remove endogenous OT. They were then incubated in 50 pM 125I-OVTA (2200 Ci/mmol; PerkinElmer; Boston, MA), a selective, radiolabeled OXTR ligand, for one hour. Unbound 125I-OVTA was then washed away with Tris-$MgCl_2$ buffer (50 mM Tris plus 2% MgCl2, pH 7.4) and sections were air dried. Sections were exposed to BioMax MR film (Kodak; Rochester, New York) for five days. Digital images were obtained with a light box and a Cannon camera (Cannon 6D MarkII, Japan). The brightness and contrast of representative images were equally adjusted for all autoradiography images within a panel using Adobe Photoshop.

Fluorescent RNAscope *in situ* hybridization for *Oxtr* mRNA localization

RNAscope Multiplex Fluorescent Reagent Kit v2 (Advanced Cell Diagnostics, Newark, California; Cat. No. 323270) was used according to the manufacturer's instructions.

Adjacent sections to those utilized for I-125 OVTA receptor binding autoradiography were used. Briefly, sections were thawed and fixed in 10% neutral buffered formalin for 15 minutes followed by treatment with hydrogen peroxide for 10 minutes and RNAscope Protease IV for 30 minutes. Probes specific to prairie vole *Oxtr* mRNA (Cat. No. 500721) were then applied and allowed to hybridize for two hours at 40 °C. After three amplification steps, hybridized probes were labelled with horseradish peroxidase (HRP), and TSA Vivid Dye 570 fluorophore. Sections were counterstained with DAPI for nuclei labeling and coverslipped with ProLong Gold Antifade Mountant (ThermoFisher Scientific; Waltham, Massachusetts). Negative controls were performed using a bacterial dapB probe (Cat. No. 310043), which did not exhibit any nonspecific labeling.

Fluorescent RNAscope images were acquired using a Keyence BZ-X710 microscope. Whole sections were captured with 10x objective lens in two channels (red and blue), and images were stitched together using Keyence BZX Analyzer Software. Brightness and contrast of the images were adjusted using Photoshop (Adobe; San Jose, California).

Quantification of *Oxtr* mRNA expression by qRT-PCR

Real-time quantitative polymerase chain reaction (RT-qPCR) using an Applied Biosystems 7500 Real-Time PCR system was used to quantify *Oxtr* mRNA expression levels in different brain regions of Koi lines. Total RNA of different brain regions was isolated using the RNeasy extraction kit (Qiagen, Germantown, US), and cDNA was synthesized after Deoxyribonuclease I (Invitrogen, Waltham, US) treatment by using EvoScript Universal cDNA Master (Roche, Penzberg, Germany), and then quantitative RT-PCR was performed with FastStart Universal SYBR Green Master (Roche, Penzberg, Germany). The relative standard curve method was used to obtain the relative quantities of *Oxtr* expression following the manual of Applied Biosystems. To allow the

comparation between Koi lines and WT mice, the following primer pair (which can detect the expression of both *mOxtr* and pv*Oxtr*) was used: fr5'-GCCTTTCTTCTTCGTGCAGATG-3' and rv5'-ATG TAGATCCAGGGGTTGCAG-3' In addition, to specifically detect the expression of pv*Oxtr*, the primer pair fr5'-GCCTTTCTTCTTCGTGCAGATG-3 and rv5'-AAAGAGGTGGCCCGTGAAC-3' was used in the 2nd qRT-PCR experiment. GAPDH was used as the endogenous control for both experiments and was amplified by the following primer pair: fr5'-GGGTTCCTATAAATACGGACTGC-3' and rv5'-CCATTTTGT CTACGGGACGA-3'.

Samples were analyzed in triplicates. A non-template control was performed to ensure that there was no amplification of genomic DNA. All of the experimenters were blind to the genotype of the subjects.

Partner preference test (PPT)

Subjects were housed with 4 age-matched and same-sex littermates until testing at adulthood (2-5 months old). 12-14 homozygous? mice were tested for each group. Ovariectomized females were paired and cohoused with a sexually experienced adult wildtype male for 21 days before PPT test. The female was injected with estradiol benzoate (10 μg and 5 μg at 48 h and 24 h before induced mating) and progesterone (500 μg at 4–7 h before induced mating) to ensure high sexual receptivity before mating.

Mating was induced on Day 2,9 and16. PPT data was analyzed using TimeSSI1 for social interaction test system (O' Hara & Co., Ltd.). Briefly, the experimental subject was placed in a chamber, in which two pen-boxes (diameter 8cm, height10cm) were located at two diagonally opposite corners. The experimental animal was free to move throughout the chamber and the time spent in close proximity to each pen-box (stay time) is recorded using an automated mouse tracking system (Fig.4 A, B). In the habituation phase, the experimental subject was allowed to explore the chamber for 5 minutes with both pen-boxes empty. In the recognition phase, the partner stimulus animal was restricted in one pen-box, and a novel "stranger" stimulus animal was restricted in another pen-box, and the experimental subject was allowed to explore the chamber for 10 minutes. In the preference phase, the positions of the partner stimulus animal and the "stranger" stimulus animal were switched, and the experimental subject was allowed to explore the chamber for 20 minutes. To assure unbiased design, pen-box assignments were counterbalanced for the diagonal positions. All of the experimenters were blind to the genotype of the subjects.

Parental behavior test

To examine maternal behavior, we performed pup retrieval test with virgin female mice (2- to 4-months old, 15-18mice/line), following the method described in (Stolzenberg, Stevens, & Rissman, 2012) with some modifications. Briefly, 5 days prior to the behavioral testing, each subject was isolated and housed in separate home cages in the test room. Nesting material (about 1.5 g of cotton wool) was provided for nest making. The tests were conducted in the dark phase of light/dark cycle (12 hours/12 hours). On the day of the test, each subject was placed in the recording area and allowed 15 minutes for habituation. The stimulus pups (age: P2-P3) were collected from a group of donor mothers immediately before the start of the experiment. A retrieval test began with the placement of 3 stimulus pups on the side farthest form the nest, and the female's behavior was recorded by an ARNAN 4 channel security system for 15 minutes. Pup retrieval was defined as picking up the pup and bringing it to the nest. If the subject did not complete the retrieval for 3 pups in 15 minutes, the video recording time was extended to 30 minutes. The latency to retrieve each pup (1st, 2nd, 3rd) and the time spent crouching on the pups were time-stamped and calculated manually. A latency of 1800 seconds was assigned if the pup-retrieval was not completed in 30 minutes. Crouching was defined as the mouse supporting itself in a lactation-position over the pups in the nest. Crouching time on a single pup, two pups, and three pups were summed up as total crouching time. All of the experimenters were blind to the genotype of the subjects.

3D chromatin verification on Hi-C datasets of humans and mice

The 3D genome structure tracks were obtained from 4DNucleome Consortium (*https://www.4dnucleome.org/*) where datasets were systematically reanalyzed following recommended standard protocols. The datasets IDs and sample information are provided in the supplementary material (Supplementary Table 1,2). 3D Genome Browser(Wang et al., 2018) and WashU Epigenome Browser(Li et al., 2022) were employed for visualizations.

Experimental design and statistical analysis

The sample sizes were determined by G*Power 3 program (Faul, Erdfelder, Lang, & Buchner, 2007) based on pilot experiments. They are also within the range that is generally accepted in the field. All experiments were performed and analyzed blind to the genotypes and no data point was excluded. All reported sample numbers (n) represent independent biological replicates that are the numbers of tested mice or tissue. All the statistical analyses were performed by SPSS21(IBM). Mixed ANOVA was used for analyzing PPT data and pup retrieval data. Mauchly's test of sphericity was used to test whether or not the assumption of sphericity was met in repeated measures. Greenhouse-Geisser correction was applied when the sphericity was violated. Two-way ANOVA was used for analyzing qRT-PCR region specific data across different mouse lines. One-way ANOVA was used for analyzing crouching time in the parental behavioral test. If there was a significant main effect of an independent factor, post hoc test was used to do multiple comparisons. If there was a significant interaction between within-subject factor and between-subject factor, post hoc pairwise comparisons were applied to analyze the simple main effects. Bonferroni correction was used for all the post hoc tests.

Supplementary Information

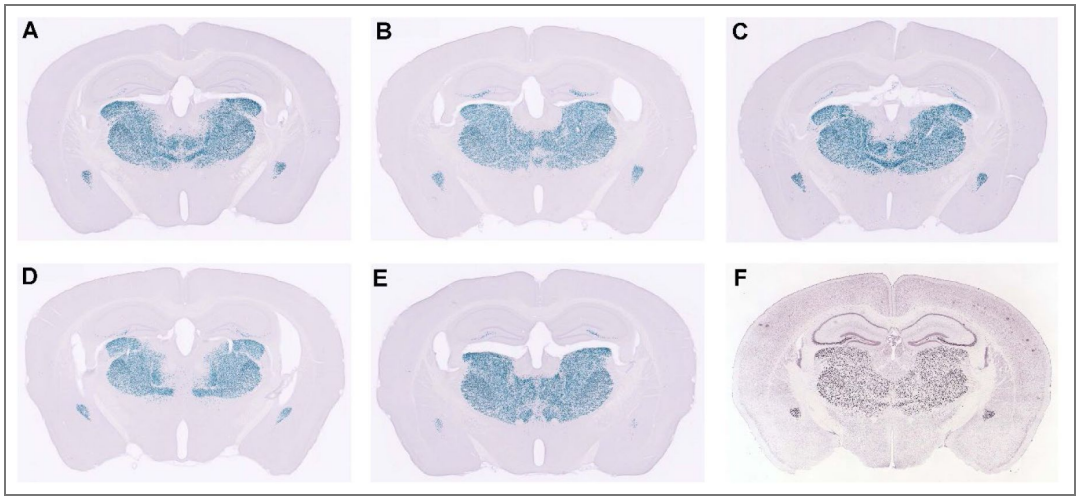

Supplementary Fig. 1. Expression pattern of the *Pkcd-Cre* BAC transgene. All five independent *Pkcd-Cre* BAC transgenic mouse lines (A–E) exhibited expression patterns that closely resembled the endogenous *Pkcd* expression, as shown by in situ hybridization (F). The *Pkcd-Cre* BAC construct was generated using the same strategy as that employed for the Koi lines, incorporating the entire intergenic regions both upstream and downstream of the *Pkcd* gene.

Supplementary Fig. 2. **Transgenic CRE mediated Lac-Z reporter gene expression in the brain of Koi lines.**

X-gal staining of the brains from the double positive (*Cre*+, *LacZ*+) offspring of Koi-5 (A-C), Koi-6 (D-F), Koi-7 (G-I), Koi-8 (J-L). Scale bar=1mm

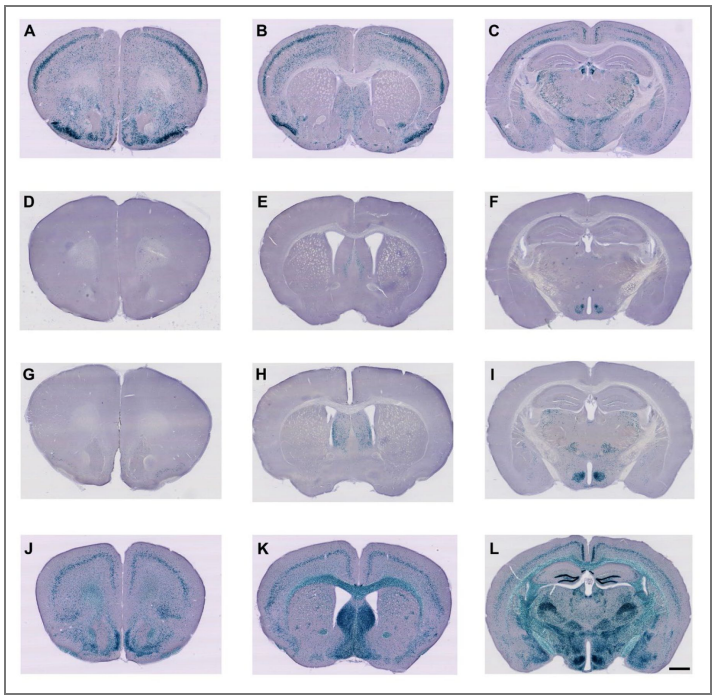

Supplementary Fig. 3. **Negative control of whole-mount mammary gland staining.**

X-gal staining of a mammary gland from (*Cre*-, *LacZ*+) offspring from heterozygous Koi-4 was shown. The lymph node showed some blue signal, indicating that the lymph node could be stained nonspecifically. All the epithelium ducts did not show any blue signal, verifying the specificity of duct labeling of X-gal staining. Scale=500um

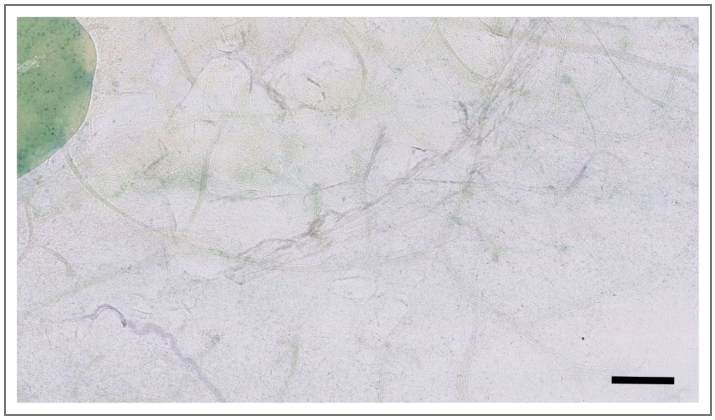

	track	ID	Cell/tissue	Organism	Restr. Enz.	Database	Database ID	Browser	Publication
Hi-C	1	Whole brain	whole brain	mm10	DNaseI	4DN	4DNFIQ48NYOW	WashU	Deng 2015
	https://4dn-open-data-public.s3.amazonaws.com/fourfront-webprod/wfoutput/60d98cc6-4583-4ebe-9c5a-77fc421ef560/4DNFIQ48NYOW.hic								
	2	NPC	NPC	mm10	DpnII	4DN	4DNFIHW8NTQX	WashU	Bonev 2017
	https://4dn-open-data-public.s3.amazonaws.com/fourfront-webprod/wfoutput/219497b5-3f35-473b-9d4e-e1cf21c69561/4DNFIHW8NTQX.hic								
	3	Cortex	cortex	mm10	MboI	4DN	4DNFII3JV8I1	WashU	Du 2017
	https://4dn-open-data-public.s3.amazonaws.com/fourfront-webprod/wfoutput/268b7d52-9655-474c-9467-8ba31bb2195c/4DNFII3JV8I1.hic								
	4	ESC	ESC	mm10	DpnII	4DN	4DNFIU8AF5ZY	WashU	Bonev 2017
	https://4dn-open-data-public.s3.amazonaws.com/fourfront-webprod/wfoutput/c2eaf9bf-9584-4cec-8685-bd74038a6c01/4DNFIU8AF5ZY.hic								
	5	Hepatocyte	hepatocyte	mm10	HindIII	4DN	4DNFIFULDMGN	WashU	Schwarzer 2017
	https://4dn-open-data-public.s3.amazonaws.com/fourfront-webprod/wfoutput/57ecaa79-5c9c-49c7-b841-0a4bf3117555/4DNFIFULDMGN.hic								
	6	Sperm	sperm	mm10	MboI	4DN	4DNFIN8F14CS	WashU	Du 2017
	https://4dn-open-data-public.s3.amazonaws.com/fourfront-webprod/wfoutput/27f54fcb-54fe-41a4-b25a-2f8944c89044/4DNFIN8F14CS.hic								

	Fig	Regions	Genes
WashU	A	chr6:104149809-119528368	Oxtr
	B	chr2:121804885-139358632	Oxt

Supplementary Table 1. The datasets IDs and sample information for mouse 3D chromatin verification

The database source of each mouse sample, analysis and visualization tool information, and the region analyzed was listed.

Data availability

Original data created for the study are available in a persistent repository as follows: Repository Name and DOI/accession number(s): zhang, qi, "Dataset - Hi-c analysis for Oxtr and Oxt", Mendeley Data, V1, doi: 10.17632/jdn6z5m6zs.1 zhang, qi, "Dataset for the analysis of koi mice", Mendeley Data, V1, doi: 10.17632/fjztcwtj2m.1

Acknowledgements

This work was supported by the RIKEN Incentive Research Project (100226201701100443) to Q.Z., the Brain Science Project, Center for novel science initiatives, National institutes of natural sciences (BS291003) to Q.Z., the RIKEN Aging Project (10026-201701100263-340120) to Q.Z., the JSPS Kakenhi Grant-in-Aid for Young Scientists (17K18362) to Q.Z., the JSPS Kakenhi Grant-in-Aid for Challenging Research (19K21807) to Q.Z., the JSPS Kakenhi Grant-in-Aid for Challenging Research (22K19478)to Q.Z., the JSPS Kakenhi Grant-in-Aid for Scientific Research (25K10198) to Q.Z., the Takeda Medical Research Grant to Q.Z., the International Education and Research Laboratory Program of University of Tsukuba to L.Y. and Q.Z.. We thank Dr. Katsuhiko Nishimori (Tohoku University and Fukushima Medical University, Japan) for providing *mOxtr*-Ires-Cre knock-in line and *mOxtr*-/- mutant line; Dr. Cary Lai (Indiana University, USA), Dr. Takuji Iwasato(National Institute of Genetics, Japan) and Dr. Seiya Mizuno(University of Tsukuba, Japan) for their advice on BAC vector construction; Dr. Volkhard Maeckel (CERN, Switzerland) for helping with image capturing; Dr. Yong Zhang (Tongji University, China) for the stimulating discussion about 3D chromatin structure, and we thank the Laboratory of Animal Resource Center of University of Tsukuba for pronuclear injection.

Additional information

Author Contributions

Q.Z. and L.Y. conceived and designed the study. Q.Z., M.T., L.N., K.I., L.K., M.P., Y.N., M.S., and T.S. performed experiments. Q.Z., M.T., L.N., K.I., L.K., M.P., and K.N. analyzed data. S.I. provided guidance and facilities for transgene vector construction. Q.Z. and L.Y. supervised the project and wrote the manuscript. All authors contributed to discussion and approved the final version.

Funding

Funder	Grant reference number	Author
MEXT | RIKEN	100226201701100443	Qi Zhang
MEXT | RIKEN	10026-201701100263-340120	Qi Zhang
MEXT | Japan Society for the Promotion of Science (JSPS)	25K10198	Qi Zhang
MEXT | Japan Society for the Promotion of Science (JSPS)	22K19478	Qi Zhang
MEXT | Japan Society for the Promotion of Science (JSPS)	19K21807	Qi Zhang
MEXT | Japan Society for the Promotion of Science (JSPS)	17K18362	Qi Zhang
Takeda Medical Research Foundation	Medical Research Grant	Qi Zhang
University of Tsukuba	International Program for Research and Education	Larry J Young

Author ORCID iDs

Kenta Nakai: https://orcid.org/0000-0002-8721-8883

Qi Zhang: https://orcid.org/0009-0005-4616-7791

References

Ahern T. H., Olsen S., Tudino R., Beery A. K (2021) Natural variation in the oxytocin receptor gene and rearing interact to influence reproductive and nonreproductive social behavior and receptor binding. *Psychoneuroendocrinology* **128**:105209 https://doi.org/10.1016/j.psyneuen.2021.105209 | PubMed

Amadei E. A., Johnson Z. V., Jun Kwon Y., Shpiner A. C., Saravanan V., Mays W. D., ..., Liu R. C. (2017) Dynamic corticostriatal activity biases social bonding in monogamous female prairie voles. *Nature* **546**:297-301 https://doi.org/10.1038/nature22381 | PubMed

Barrett C. E., Arambula S. E., Young L. J (2015) The oxytocin system promotes resilience to the effects of neonatal isolation on adult social attachment in female prairie voles. *Transl Psychiatry* **5**:e606 https://doi.org/10.1038/tp.2015.73 | PubMed

Beagan J. A., Phillips-Cremins J. E (2020) On the existence and functionality of topologically associating domains. *Nature Genetics* **52**:8-16 https://doi.org/10.1038/s41588-019-0561-1 | PubMed

Beil J., Fairbairn L., Pelczar P., Buch T (2012) Is BAC transgenesis obsolete? State of the art in the era of designer nucleases. *J Biomed Biotechnol* **2012**:308414 https://doi.org/10.1155/2012/308414 | PubMed

Bian Q., Belmont A. S (2010) BAC TG-EMBED: one-step method for high-level, copy-number-dependent, position-independent transgene expression. *Nucleic Acids Research* **38**:e127-e127 https://doi.org/10.1093/nar/gkq178 | PubMed

Carcea I., Caraballo N. L., Marlin B. J., Ooyama R., Riceberg J. S., Mendoza Navarro J. M., ..., Froemke R. C. (2021) Oxytocin neurons enable social transmission of maternal behaviour. *Nature* **596**:553-557 https://doi.org/10.1038/s41586-021-03814-7 | PubMed

Chandler K. J., Chandler R. L., Broeckelmann E. M., Hou Y., Southard-Smith E. M., Mortlock D. P (2007) Relevance of BAC transgene copy number in mice: transgene copy number variation across multiple transgenic lines and correlations with transgene integrity and expression. *Mamm Genome* **18**:693-708 https://doi.org/10.1007/s00335-007-9056-y | PubMed

Chen Z., Han Y., Ma Z., Wang X., Xu S., Tang Y., ..., Zhan Y. (2024) A prefrontal-thalamic circuit encodes social information for social recognition. *Nature Communications* **15**:1036 https://doi.org/10.1038/s41467-024-45376-y | PubMed

Crook Z. R., Housman D (2011) Huntington's disease: can mice lead the way to treatment?. *Neuron* **69**:423-435 https://doi.org/10.1016/j.neuron.2010.12.035 | PubMed

Dekker J., Rippe K., Dekker M., Kleckner N (2002) Capturing chromosome conformation. *Science* **295**:1306-1311 https://doi.org/10.1126/science.1067799 | PubMed

Dixon J. R., Selvaraj S., Yue F., Kim A., Li Y., Shen Y., ..., Ren B. (2012) Topological domains in mammalian genomes identified by analysis of chromatin interactions. *Nature* **485**:376-380 https://doi.org/10.1038/nature11082 | PubMed

Faul F., Erdfelder E., Lang A. G., Buchner A (2007) G*Power 3: a flexible statistical power analysis program for the social, behavioral, and biomedical sciences. *Behav Res Methods* **39**:175-191 https://doi.org/10.3758/bf03193146 | PubMed

Ferrante R. J (2009) Mouse models of Huntington's disease and methodological considerations for therapeutic trials. *Biochimica et Biophysica Acta (BBA) - Molecular Basis of Disease* **1792**:506-520 https://doi.org/10.1016/j.bbadis.2009.04.001 | PubMed

Froemke R. C., Young L. J (2021) Oxytocin, Neural Plasticity, and Social Behavior. *Annu Rev Neurosci* **44**:359-381 https://doi.org/10.1146/annurev-neuro-102320-102847 | PubMed

Gerfen C. R., Paletzki R., Heintz N (2013) GENSAT BAC cre-recombinase driver lines to study the functional organization of cerebral cortical and basal ganglia circuits. *Neuron* **80**:1368-1383 https://doi.org/10.1016/j.neuron.2013.10.016 | PubMed

Gibcus Johan H., Dekker J (2013) The Hierarchy of the 3D Genome. *Molecular Cell* **49**:773-782 https://doi.org/10.1016/j.molcel.2013.02.011 | PubMed

Gilligan P., Brenner S., Venkatesh B (2003) Neurone-specific expression and regulation of the pufferfish isotocin and vasotocin genes in transgenic mice. *J Neuroendocrinol* **15**:1027-1036 https://doi.org/10.1046/j.1365-2826.2003.01090.x | PubMed

Gong S., Doughty M., Harbaugh C. R., Cummins A., Hatten M. E., Heintz N., Gerfen C. R (2007) Targeting Cre recombinase to specific neuron populations with bacterial artificial chromosome constructs. *J Neurosci* **27**:9817-9823 https://doi.org/10.1523/jneurosci.2707-07.2007 | PubMed

Gong S., Zheng C., Doughty M. L., Losos K., Didkovsky N., Schambra U. B., ..., Heintz N. (2003) A gene expression atlas of the central nervous system based on bacterial artificial chromosomes. *Nature* **425**:917-925 https://doi.org/10.1038/nature02033 | PubMed

Grinevich V., Knobloch-Bollmann H. S., Eliava M., Busnelli M., Chini B (2016) Assembling the Puzzle: Pathways of Oxytocin Signaling in the Brain. *Biol Psychiatry* **79**:155-164 https://doi.org/10.1016/j.biopsych.2015.04.013 | PubMed

Heintz N (2004) Gene Expression Nervous System Atlas (GENSAT). *Nature Neuroscience* **7**:483-483 https://doi.org/10.1038/nn0504-483 | PubMed

Hidema S., Fukuda T., Hiraoka Y., Mizukami H., Hayashi R., Otsuka A., ..., Nishimori K. (2016) Generation of Oxtr cDNA(HA)-Ires-Cre Mice for Gene Expression in an Oxytocin Receptor Specific Manner. *J Cell Biochem* **117**:1099-1111 https://doi.org/10.1002/jcb.25393 | PubMed

Inoue K., Ford C. L., Horie K., Young L. J (2022) Oxytocin receptors are widely distributed in the prairie vole (Microtus ochrogaster) brain: Relation to social behavior, genetic polymorphisms, and the dopamine system. *Journal of Comparative Neurology* **530**:2881-2900 https://doi.org/10.1002/cne.25382 | PubMed

Jurek B., Neumann I. D (2018) The Oxytocin Receptor: From Intracellular Signaling to Behavior. *Physiological reviews* **98**:1805-1908 https://doi.org/10.1152/physrev.00031.2017 | PubMed

Kandasamy L. C., Tsukamoto M., Banov V., Tsetsegee S., Nagasawa Y., Kato M., ..., Zhang Q. (2021) Limb-clasping, cognitive deficit and increased vulnerability to kainic acid-induced seizures in neuronal glycosylphosphatidylinositol deficiency mouse models. *Human Molecular Genetics* **30**:758-770 https://doi.org/10.1093/hmg/ddab052 | PubMed

Kappel J. M., Förster D., Slangewal K., Shainer I., Svara F., Donovan J. C., ..., Larsch J. (2022) Visual recognition of social signals by a tectothalamic neural circuit. *Nature* **608**:146-152 https://doi.org/10.1038/s41586-022-04925-5 | PubMed

Kim J. H., Lee S. R., Li L. H., Park H. J., Park J. H., Lee K. Y., ..., Choi S. Y. (2011) High cleavage efficiency of a 2A peptide derived from porcine teschovirus-1 in human cell lines, zebrafish and mice. *PloS one* **6**:e18556 https://doi.org/10.1371/journal.pone.0018556 | PubMed

King L. B., Walum H., Inoue K., Eyrich N. W., Young L. J (2016) Variation in the Oxytocin Receptor Gene Predicts Brain Region-Specific Expression and Social Attachment. *Biol Psychiatry* **80**:160-169 https://doi.org/10.1016/j.biopsych.2015.12.008 | PubMed

Leng G., Ludwig M (2008) Neurotransmitters and peptides: whispered secrets and public announcements. *J Physiol* **586**:5625-5632 https://doi.org/10.1113/jphysiol.2008.159103 | PubMed

Li D., Purushotham D., Harrison J. K., Hsu S., Zhuo X., Fan C., ..., Wang T. (2022) WashU Epigenome Browser update 2022. *Nucleic Acids Research* **50**:W774-W781 https://doi.org/10.1093/nar/gkac238 | PubMed

Lieberman-Aiden E., van Berkum N. L., Williams L., Imakaev M., Ragoczy T., Telling A., ..., Dekker J. (2009) Comprehensive Mapping of Long-Range Interactions Reveals Folding Principles of the Human Genome. *Science* **326**:289-293 https://doi.org/10.1126/science.1181369 | PubMed

Mack K. L., Campbell P., Nachman M. W (2016) Gene regulation and speciation in house mice. *Genome Res* **26**:451-461 https://doi.org/10.1101/gr.195743.115 | PubMed

Marlin B. J., Mitre M., D'Amour J A., Chao M. V., Froemke R. C (2015) Oxytocin enables maternal behaviour by balancing cortical inhibition. *Nature* **520**:499-504 https://doi.org/10.1038/nature14402 | PubMed

McGraw L. A., Davis J. K., Lowman J. J., ten Hallers B. F. H., Koriabine M., Young L. J., ..., Thomas J. W. (2010) Development of genomic resources for the prairie vole (Microtus ochrogaster): construction of a BAC library and vole-mouse comparative cytogenetic map. *BMC Genomics* **11**:70 https://doi.org/10.1186/1471-2164-11-70 | PubMed

McGraw L. A., Davis J. K., Thomas P. J., Young L. J., Thomas J. W (2012) BAC-based sequencing of behaviorally-relevant genes in the prairie vole. *PloS one* **7**:e29345 https://doi.org/10.1371/journal.pone.0029345 | PubMed

Mitre M., Marlin B. J., Schiavo J. K., Morina E., Norden S. E., Hackett T. A., ..., Froemke R. C. (2016) A Distributed Network for Social Cognition Enriched for Oxytocin Receptors. *J Neurosci* **36**:2517-2535 https://doi.org/10.1523/jneurosci.2409-15.2016 | PubMed

Newmaster K. T., Nolan Z. T., Chon U., Vanselow D. J., Weit A. R., Tabbaa M., ..., Kim Y. (2020) Quantitative cellular-resolution map of the oxytocin receptor in postnatally developing mouse brains. *Nature Communications* **11**:1885 https://doi.org/10.1038/s41467-020-15659-1 | PubMed

Olazábal D. E., Young L. J (2006) Oxytocin receptors in the nucleus accumbens facilitate "spontaneous" maternal behavior in adult female prairie voles. *Neuroscience* **141**:559-568 https://doi.org/10.1016/j.neuroscience.2006.04.017 | PubMed

Osada N., Miyagi R., Takahashi A (2017) Cis- and Trans-regulatory Effects on Gene Expression in a Natural Population of Drosophila melanogaster. *Genetics* **206**:2139-2148 https://doi.org/10.1534/genetics.117.201459 | PubMed

Parmaksiz D., Kim Y (2025) Navigating Central Oxytocin Transport: Known Realms and Uncharted Territories. *Neuroscientist* **31**:234-261 https://doi.org/10.1177/10738584241268754 | PubMed

Phelps S. M., Young L. J (2003) Extraordinary diversity in vasopressin (V1a) receptor distributions among wild prairie voles (Microtus ochrogaster): patterns of variation and covariation. *J Comp Neurol* **466**:564-576 https://doi.org/10.1002/cne.10902 | PubMed

Rajderkar S., Barozzi I., Zhu Y., Hu R., Zhang Y., Li B., ..., Pennacchio L. A. (2023) Topologically associating domain boundaries are required for normal genome function. *Communications Biology* **6**:435 https://doi.org/10.1038/s42003-023-04819-w | PubMed

Rangel M. J., Baldo M. V. C., Canteras N. S (2018) Influence of the anteromedial thalamus on social defeat-associated contextual fear memory. *Behavioural Brain Research* **339**:269-277 https://doi.org/10.1016/j.bbr.2017.10.038 | PubMed

Rigney N., de Vries G. J., Petrulis A., Young L. J. (2022) Oxytocin, Vasopressin, and Social Behavior: From Neural Circuits to Clinical Opportunities. *Endocrinology* **163** https://doi.org/10.1210/endocr/bqac111 | PubMed

Rogers Flattery C. N., Coppeto D. J., Inoue K., Rilling J. K., Preuss T. M., Young L. J. (2022) Distribution of brain oxytocin and vasopressin V1a receptors in chimpanzees (Pan troglodytes): comparison with humans and other primate species. *Brain Struct Funct* **227**:1907-1919 https://doi.org/10.1007/s00429-021-02369-7 | PubMed

Ross H. E., Freeman S. M., Spiegel L. L., Ren X., Terwilliger E. F., Young L. J (2009) Variation in oxytocin receptor density in the nucleus accumbens has differential effects on affiliative behaviors in monogamous and polygamous voles. *J Neurosci* **29**:1312-1318 https://doi.org/10.1523/jneurosci.5039-08.2009 | PubMed

Ross H. E., Young L. J (2009) Oxytocin and the neural mechanisms regulating social cognition and affiliative behavior. *Front Neuroendocrinol* **30**:534-547 https://doi.org/10.1016/j.yfrne.2009.05.004 | PubMed

Schmidt E. F., Kus L., Gong S., Heintz N (2013) BAC transgenic mice and the GENSAT database of engineered mouse strains. *Cold Spring Harb Protoc* **2013** https://doi.org/10.1101/pdb.top073692 | PubMed

Shenoy S. A., Zheng S., Liu W., Dai Y., Liu Y., Hou Z., ..., Li C. (2022) A novel and accurate full-length HTT mouse model for Huntington's disease. *eLife* **11**:e70217 https://doi.org/10.7554/eLife.70217 | PubMed

Shi X., Ng D. W. K., Zhang C., Comai L., Ye W., Jeffrey Chen Z (2012) Cis- and trans-regulatory divergence between progenitor species determines gene-expression novelty in Arabidopsis allopolyploids. *Nature Communications* **3**:950 https://doi.org/10.1038/ncomms1954 | PubMed

Signor S. A., Nuzhdin S. V (2018) The Evolution of Gene Expression in cis and trans. *Trends Genet* **34**:532-544 https://doi.org/10.1016/j.tig.2018.03.007 | PubMed

Skuse D. H., Lori A., Cubells J. F., Lee I., Conneely K. N., Puura K., ..., Young L. J. (2014) Common polymorphism in the oxytocin receptor gene (*OXTR*) is associated with human social recognition skills. *Proceedings of the National Academy of Sciences* **111**:1987-1992 https://doi.org/10.1073/pnas.1302985111 | PubMed

Smirnov A., Fishman V., Yunusova A., Korablev A., Serova I., Skryabin B. V., ..., Battulin N. (2019) DNA barcoding reveals that injected transgenes are predominantly processed by homologous recombination in mouse zygote. *Nucleic Acids Research* **48**:719-735 https://doi.org/10.1093/nar/gkz1085 | PubMed

Stolzenberg D. S., Stevens J. S., Rissman E. F (2012) Experience-facilitated improvements in pup retrieval; evidence for an epigenetic effect. *Horm Behav* **62**:128-135 https://doi.org/10.1016/j.yhbeh.2012.05.012 | PubMed

Suster M. L., Abe G., Schouw A., Kawakami K (2011) Transposon-mediated BAC transgenesis in zebrafish. *Nature Protocols* **6**:1998-2021 https://doi.org/10.1038/nprot.2011.416 | PubMed

Taguchi T., Ikuno M., Hondo M., Parajuli L. K., Taguchi K., Ueda J., ..., Takahashi R. (2019) α-Synuclein BAC transgenic mice exhibit RBD-like behaviour and hyposmia: a prodromal Parkinson's disease model. *Brain* **143**:249-265 https://doi.org/10.1093/brain/awz380 | PubMed

Takayanagi Y., Yoshida M., Bielsky I. F., Ross H. E., Kawamata M., Onaka T., ..., Nishimori K. (2005) Pervasive social deficits, but normal parturition, in oxytocin receptor-deficient mice. *Proceedings of the National Academy of Sciences* **102**:16096-16101 https://doi.org/10.1073/pnas.0505312102 | PubMed

Theofanopoulou C., Andirkó A., Boeckx C., Jarvis E. D (2022) Oxytocin and vasotocin receptor variation and the evolution of human prosociality. *Comprehensive Psychoneuroendocrinology* **11**:100139 https://doi.org/10.1016/j.cpnec.2022.100139 | PubMed

Venkatesh B., Si-Hoe S. L., Murphy D., Brenner S (1997) Transgenic rats reveal functional conservation of regulatory controls between the Fugu isotocin and rat oxytocin genes. *Proc Natl Acad Sci U S A* **94**:12462-12466 https://doi.org/10.1073/pnas.94.23.12462 | PubMed

Walum H., Young L. J (2018) The neural mechanisms and circuitry of the pair bond. *Nat Rev Neurosci* **19**:643-654 https://doi.org/10.1038/s41583-018-0072-6 | PubMed

Walum H., Young L. J (2018) The neural mechanisms and circuitry of the pair bond. *Nature Reviews Neuroscience* **19**:643-654 https://doi.org/10.1038/s41583-018-0072-6 | PubMed

Wang Y., Song F., Zhang B., Zhang L., Xu J., Kuang D., ..., Yue F. (2018) The 3D Genome Browser: a web-based browser for visualizing 3D genome organization and long-range chromatin interactions. *Genome Biol* **19**:151 https://doi.org/10.1186/s13059-018-1519-9 | PubMed

Wendt K. S., Yoshida K., Itoh T., Bando M., Koch B., Schirghuber E., ..., Peters J. M. (2008) Cohesin mediates transcriptional insulation by CCCTC-binding factor. *Nature* **451**:796-801 https://doi.org/10.1038/nature06634 | PubMed

Wolff M., Vann S. D (2019) The Cognitive Thalamus as a Gateway to Mental Representations. *J Neurosci* **39**:3-14 https://doi.org/10.1523/jneurosci.0479-18.2018 | PubMed

Xiao J. Y., Hafner A., Boettiger A. N (2021) How subtle changes in 3D structure can create large changes in transcription. *eLife* **10**:e64320 https://doi.org/10.7554/eLife.64320 | PubMed

Yang X. W., Lu X.-H (2008) Chapter 19 - The Bac Transgenic Approach to Study Parkinson's Disease in Mice. In: Nass R., Przedborski S. (Eds). *Parkinson's Disease* San Diego: Academic Press. pp. 247-268 https://doi.org/10.1016/b978-0-12-374028-1.00019-1

Young L. J., Crews D (1995) Comparative neuroendocrinology of steroid receptor gene expression and regulation: Relationship to physiology and behavior. *Trends Endocrinol Metab* **6**:317-323 https://doi.org/10.1016/1043-2760(95)00175-1 | PubMed

Young L. J., Zhang Q. I (2021) On the Origins of Diversity in Social Behavior. *The Japanese Journal of Animal Psychology* https://doi.org/10.2502/janip.71.1.4

Zhang Q., Sano C., Masuda A., Ando R., Tanaka M., Itohara S (2016) Netrin-G1 regulates fear-like and anxiety-like behaviors in dissociable neural circuits. *Scientific Reports* **6**:28750 https://doi.org/10.1038/srep28750 | PubMed

Peer reviews

Reviewer #1 (Public review):

Summary:

The manuscript by Tsukamoto et al. describes a compelling approach to understanding whether inter-species differences in social behavior might emerge from differential expression patterns of the oxytocin receptor (Oxtr) in the brain. To this end, they genetically engineer BAC transgenic mouse lines with insertions of a large construct incorporating prairie vole Oxtr gene and surrounding regulatory elements. They name these lines Koi lines. They first evaluate if prairie vole-like Oxtr expression is reproduced in the Koi mouse lines, and they find heterogenous patterns across different lines that do not depend on the number of insertions. While they found that Koi mice can reproduce vole-like expression in PFC, NAc, and BLA, the reproduction was never complete: one Koi line had NAc and mPFC expression, another had BLA expression, etc. They confirmed major expression patterns across 3 methods: crossing with LacZ reporter line, in situ hybridization, and ligand binding (autoradiography). To determine the expression pattern of the BAC insert but not endogenous Oxtr, the authors generated new mouse lines by crossing Koi lines with Oxtr -/- line. Importantly, they found that Oxtr expression pattern in the mammary gland was similar across all lines, and wild-type mice.

The authors used Koi:Oxtr-/- lines to test social behavior, specifically partner preference (a behavior specific to prairie voles) and maternal behavior. They find that different Koi lines showed different changes in these behaviors compared to wild-type mice. Moreover, while some lines showed changes in partner preference, others seemed to show changes in maternal behavior. For one of the lines (Koi4), the partner preference and the maternal behavior were incongruent.

The manuscript then hypothesizes that the Oxtr gene is positioned in different 3D chromatin structures across species and across tissues, leading to more rigid expression in the mammary glands, but more flexible expression patterns in the brain.

Strengths:

This study has major implications in the field of oxytocin research, and more broadly in the field of neuromodulation. It is novel, bold, and rigorous.

Weaknesses:

(1) The expression in the brain and mammary gland (Figure 2) was not quantified, preventing a more objective conclusion that the brain has flexible expression and mammary gland expression is rigid.

(2) In Figure 7, a similar heatmap for the mammary gland is missing.

(3) Partner preference in males was not tested.

(4) It is unclear if in the behavioral testing the stimulus animals were the same genotype as the focal female or were wild-types. This could have an impact on the behavioral outcome.

https://doi.org/10.7554/eLife.109080.1.sa1

Reviewer #2 (Public review):

Summary:

This is a bold and important study and addresses an important question in the field: how species-specific variation in brain oxytocin receptor expression relates to differences in social behavior.

Tsukamoto et al. generated eight independent transgenic mouse lines (Koi lines) carrying a bacterial artificial chromosome (BAC) encompassing the prairie vole Oxtr locus along with flanking intergenic regions, with the goal of probing the behavioral consequences of species-specific variation in brain Oxtr expression. Across these "volized" lines, the authors claim conserved Oxtr expression in the mammary gland but strikingly divergent patterns of brain expression, none of which fully recapitulate endogenous prairie vole Oxtr distribution, and instead exhibit expression patterns that diverge from both mouse and prairie vole brain Oxtr distribution. Nevertheless, some lines exhibit partial overlap with vole Oxtr expression pattern reported in the literature within specific brain regions, and one line displays partner preference behavior reminiscent of prairie voles. The authors further report line-dependent differences in maternal pup retrieval and crouching behaviors, which they interpret as evidence that variation in brain Oxtr expression can drive variation in social behaviors. Together with analyses of topologically associating domain (TAD) architecture, the authors conclude that brain, but not peripheral- Oxtr expression, is shaped by distal regulatory elements beyond the BAC insert, and propose that such regulatory flexibility underlies evolutionary diversification of social behavior.

Strengths:

A particular strength of the study is the generation of multiple independent transgenic lines, which provides a valuable resource for probing regulatory influences on Oxtr expression.

Weaknesses:

While the study addresses an important question, I have several methodological and conceptual concerns regarding the study in its current form. Some aspects of the study fall outside my primary area of expertise, and I am therefore not in a position to fully evaluate the technical difficulty or rigor of those components, or to judge whether my suggestions would be feasible to implement. I defer to reviewers with relevant expertise for a more detailed assessment of these aspects.

(1) Each independent Koi line exhibits a distinct brain expression pattern that differs from both wild-type mouse and prairie vole Oxtr expression, complicating the interpretation of the results. The manuscript does not include a direct comparison of brain Oxtr expression patterns in these transgenic lines with those of prairie voles. Instead, expression similarity is inferred primarily from regional localization and compared indirectly with prior literature (Figures 2-5). For those lines that show partial resemblance to prairie vole Oxtr expression patterns, the authors do not assess whether Oxtr-expressing neurons share comparable anatomical projections or transcriptomic identity with prairie vole Oxtr-expressing neurons. Quantification of expression remains largely descriptive, illustrating expression patterns

(Figure 2), OXTR protein distribution (Figure 3; images are difficult to evaluate due to low contrast), or Oxtr mRNA levels across selected brain regions in Koi lines, wild-type mice, and mOxtr-/- mice (Figures 4-5), without directly testing similarity to prairie vole expression. In addition, whole-brain expression data are lacking, with analyses restricted to selected sections. While such analyses may be beyond the scope of the present study, these limitations nonetheless complicate interpretation of the central question - namely, whether the observed behavioral phenotypes arise from vole-like Oxtr circuits rather than from distinct, line-specific expression configurations.

(2) The authors state that Oxtr expression in the mammary gland is similar across all Koi lines and the mOxtr-IRES-Cre knock-in line. However, the images presented in Figure 2 appear to show differences in anatomical detail across lines, and no quantitative analysis is provided to support the claim of equivalence.

(3) The conclusion that integration site rather than copy number determines the observed BAC transgene expression patterns (Lines 202-203) is not fully supported by the data. First, the authors did not compare multiple copy numbers at the same genomic insertion site, making it impossible to disentangle copy-number effects from position effects. Second, BAC copy number does not necessarily scale linearly with expression; higher copy numbers can have a repressive effect on gene expression (Garrick et al, Nat Genet, 1998).

(4) While I am not an expert in TAD analysis, the observed differences in 3D architecture around Oxtr are consistent with a role for long-range regulatory interactions. However, these analyses appear largely descriptive and correlative, and establishing a causal contribution of 3D chromatin organization to Oxtr regulation by distal elements would likely require direct perturbation of TAD boundaries or looping interactions. I recognize that such experiments may be beyond the scope of the present study, but clarifying this limitation in the interpretation would be helpful.

https://doi.org/10.7554/eLife.109080.1.sa0

Author response:

Thank you very much for your careful evaluation of our manuscript entitled *"Cross-Species BAC Transgenesis Reveals Long-Range Regulation Drives Variation in Brain Oxytocin Receptor Expression and Social Behaviors."* We sincerely appreciate the insightful and constructive comments from both reviewers.

We are particularly encouraged by the positive assessment that our study provides a useful experimental framework and resource for understanding how regulatory variation contributes to diversity in brain expression patterns and social behaviors. We have carefully considered all comments and outline below the key revisions we will implement in the revised manuscript.

Conceptual clarification: We will clarify the conceptual framework of the study. While our initial aim was to test whether prairie vole regulatory elements could recapitulate vole-like *Oxtr* expression patterns in mice, the generation of multiple independent Koi lines revealed that such expression is not faithfully reproduced but instead varies across lines. This observation led us to refocus the study on how regulatory architecture gives rise to diverse expression patterns and their functional consequences. Accordingly, we will revise the manuscript to emphasize that the goal is not to reconstruct prairie vole circuits, but to test how variation in *Oxtr* expression distribution drives variation in social behaviors.

Quantification of expression patterns: We will include quantitative analyses of *Oxtr* expression in both brain and mammary gland tissues. These additions will provide an objective basis for comparing tissue-specific expression and support the conclusion that brain

expression is more variable, whereas mammary gland expression is broadly conserved. We will include qRT-PCR data to support mammary gland comparisons.

Behavioral interpretation: We will clarify that the behavioral analyses are designed to assess how distinct *Oxtr* expression patterns influence social behaviors within a controlled mouse system, rather than to directly replicate prairie vole phenotypes. We will refine the manuscript to clearly distinguish between partial resemblance to prairie vole expression and the broader goal of linking regulatory variation to behavioral diversity.

Technical clarification and limitations: We will revise the manuscript to more carefully interpret the roles of genomic integration site and transgene copy number, noting that while integration site likely plays a major role, contributions from copy number cannot be excluded. In addition, we will explicitly acknowledge that our analyses of 3D chromatin architecture are correlative in nature, and that establishing causality would require direct perturbation of chromatin structure, which is beyond the scope of the current study.

Presentation improvements: We will improve figure clarity, include representative reference images from prairie vole brain to facilitate qualitative comparison, and refine descriptions in the Results and Methods sections to enhance clarity and readability.

We thank the reviewers again for their insightful and constructive feedback, which we believe will significantly strengthen the manuscript. We look forward to submitting a revised version incorporating these improvements.

https://doi.org/10.7554/eLife.109080.1.sa3